

1 **The Transient Variation of the Complexes of the Low Latitude Ionosphere within the**
2 **Equatorial Ionization Anomaly Region of Nigeria.**

3 **A. B. Rabi^{1,2}, B. O. Ogunsua¹, I. A. Fuwape¹ and J. A. Laoye³**

4 [1] {Space Physics Laboratory, Department of Physics, Federal University of Technology,
5 Akure, Nigeria}

6 [2]{Centre for Atmospheric Research, National Space Research and Development Agency,
7 Anyigba, Nigeria}

8 [3] {Department of Physics, Olabisi Onabanjo University, Ago-Iwoye, Nigeria}

9

10 Correspondence to: B. O. Ogunsua (iobogunsua@futa.edu.ng)

11

12 **Abstract**

13 The quest to find an index for proper characterization and description of the dynamical response
14 of the ionosphere to external influences and its various internal irregularities has led to the study
15 of the day to day variations of the chaoticity and dynamical complexity of the ionosphere. This
16 study was conducted using Global Positioning System (GPS) Total Electron Content (TEC) time
17 series, measured in the year 2011, from 5 GPS receiver stations in Nigeria which lies within the
18 Equatorial Ionization Anomaly region. The nonlinear aspect of the TEC time series were
19 obtained by detrending the data. The detrended TEC time series were subjected to various
20 analyses to obtain the phase space reconstruction and to compute the chaotic quantifiers which
21 are Lyapunov exponents LE, correlation dimension, and Tsallis entropy for the study of
22 dynamical complexity. Considering all the days of the year the daily/transient variations show no
23 definite pattern for each month but day to day values of Lyapunov exponent for the entire year
24 show a wavelike semiannual variation pattern with lower values around March, April, September
25 and October. This can be seen from the correlation dimension with values between 2.7 and 3.2
26 with lower values occurring mostly during storm periods demonstrating a phase transition from
27 higher dimension during the quiet periods to lower dimension during storms for most of the
28 stations. The values of Tsallis entropy show similar variation pattern with that of Lyapunov
29 Exponent, with both quantifiers correlating within the range of 0.79 to 0.82. These results show
30 that both quantifiers can be further used together as indices in the study of the variations of the

31 dynamical complexity of the ionosphere. The presence of chaos and high variations in the
32 dynamical complexity, even at quiet periods in the ionosphere may be due to the internal
33 dynamics and inherent irregularities of the ionosphere which exhibit non-linear properties.
34 However, this inherent dynamics may be complicated by external factors like Geomagnetic
35 storms. This may be the main reason for the drop in the values of Lyapunov exponent and Tsallis
36 entropy during storms. The dynamical behavior of the ionosphere throughout the year as
37 described by these quantifiers, were discussed in this work.

38

39 **1.0 Introduction**

40 The behavior of natural systems like the ionosphere is a function of changes that occur in the
41 underlying dynamics that exists in such system. These underlying dynamics however can be
42 sometimes complex and nonlinear due to superposition of different changes in dynamical
43 variables that constitute it. However, there is no totally deterministic system in nature, because
44 all natural systems exhibit a mixture of both stochastic and deterministic properties. Although
45 few natural systems have been found to be low dimensional deterministic in the sense of the
46 theory, the concept of low-dimensional chaos has been proven to be fruitful in the understanding
47 of many complex phenomena (Hegger et al., 1999) The degree of determinism or stochasticity in
48 most natural systems is dependent on how much the system can be influenced by external
49 factors, the nature of these external factors among others .The ionosphere like every other natural
50 system possess its intrinsic dynamics and it can also be influenced by other external factors. The
51 typical characteristics of a dynamical system like the ionosphere is expected to naturally show
52 the interplay between determinism and stochasticity simply because of the fact that the
53 ionosphere which has an inherent internal dynamics is also influenced by the influx of stochastic
54 drivers like the solar wind, since it is influenced by external dynamics like every other natural
55 system. This has made pure determinism impossible in the ionosphere, a situation that is
56 common to all natural system and its surrounding.

57 The intensity of the solar wind coming into the ionosphere varies with the solar activity and this
58 can sometimes result into geomagnetic storms and substorms drive in high intensity plasma wind
59 at enormous speed and it serves as major stochastic driver leading to storm. The solar wind is
60 driven from the sun into the ionospheric system during the quiet and storm and during relatively

61 quiet periods of each month of the year. However other processes which include various factors
62 like local time variations of the neutral winds, ionization processes, production-recombination
63 rates, photoionization processes, plasma diffusion and various electrodynamics processes.
64 (Unnikrishnan, 2010). The mesosphere and the lower thermospheric dynamics as reported by
65 Kazimirovsky and Vergasova (2009) and also the influence of gravity waves as reported by
66 Sindelarova (2009) can also be of great influence on the internal dynamics of the ionosphere.

67 Therefore, it is of great importance to study the chaoticity and dynamical complexity of the
68 ionosphere and its variations in all geophysical conditions. However a good number of
69 investigations have been carried out on concept of chaos in the upper atmosphere before now
70 which includes the study on magnetospheric dynamics and the ionosphere. The study of chaos in
71 magnetospheric index time series such as AE and AL were initially carried out by (Vasiliadis et
72 al., 1990, Shan et al, 1999; Pavlos et al, 1992). These previous efforts made by the
73 aforementioned researchers has led to the development of the concept of investigating and
74 revealing the chaoticity and the complex dynamics of the ionosphere, and as a result, studies on
75 the chaoticity of the ionosphere have been conducted, by some investigators like Bhattacharyya
76 (1990) who studied chaotic behavior of ionospheric diversity fluctuation using amplitude and
77 phase scintillation data, and found the existence of low dimension chaos. Also, Wernik and Yeh
78 (1994) further revealed the chaotic behavior of the ionospheric turbulence using scintillation data
79 and numerical modeling of scintillation at high latitude. They showed that the ionospheric
80 turbulence attractor (if it exists) cannot be reconstructed from amplitude scintillation data and
81 their measured phase scintillation data adequately reproduce the assumed chaotic structure in the
82 ionosphere. Also Kumar et al., (2004) reported the evidence of chaos in the ionosphere by
83 showing the chaotic nature of the underlying dynamics of the fluctuations of TEC power
84 spectrum indicating exponential decay and the calculated positive value of Lyapunov exponent.
85 This is also supported by the results of the comparison of the chaotic characteristics of the time
86 series of variations of TEC with the pseudochaotic characteristic of the colored noise time series.
87 Xuann et al., (2006) studied chaos properties of ionospheric total electron content (TEC) using
88 TEC data from 1996 to 2004, and analyze possibility to predict it by using chaos. They found
89 the presence of chaos in the TEC measured in the study area, as indicated by the positive
90 Lyapunov exponent computed from their data. The correlation dimension was 3.6092 from their
91 estimation. They were also able to show that the TEC time series can be predicted using chaos.

92

93 Also, Unnikrishnan et al (2006a,b) have analyzed the deterministic chaos in mid latitude and
94 Unnikrishnan (2010), Unnikrishnan and Ravindran (2010), analyzed some TEC data from some
95 Indian low latitude stations for quiet period and major storm period and found in Their results the
96 presence of chaos which was indicated by a positive Lyapunov exponent, and they also inferred
97 that storm periods exhibits lower values compared to quiet periods. The dynamical complexity
98 of magnetospheric processes and the ionosphere have been studied by a number of researchers.
99 Balasis et al., (2008) investigated the dynamical complexity of the magnetosphere by using
100 Tsallis entropy as a dynamical complexity measure in D_{st} time series also Balasis et al., (2009)
101 investigated the dynamical complexity in D_{st} further by considering different entropy measures.
102 Coco et al (2011) using the information theory approach studied the dynamical changes of the
103 polar cap potential which is characteristic of the polar region ionosphere by considering three
104 cases (i) steady IMF $B_z > 0$, (ii) steady IMF $B_z < 0$ and (iii) a double rotation from negative to
105 positive and then positive to negative B_z . They observed a neat dynamical topological transition
106 when the IMF B_z turns from negative to positive and vice versa, pointing toward the possible
107 occurrence of an order/disorder phase transition, which is the counterpart of the large scale
108 convection rearrangement and of the increase of the global coherence. Further studies on the
109 chaotic behavior and nonlinear dynamics of the ionosphere over the low latitude African region
110 is however required for the improvement of our understanding and characterization of its
111 dynamical behavior. Recently Ogunsua et al (2014) studied comparatively the chaoticity of the
112 equatorial ionosphere over Nigeria using TEC data, considering five quietest day classification
113 and five most disturbed day classification. They were able to show the presence of chaos as
114 indicated the positive Lyapunov exponents and also were able to show that Tsallis entropy can
115 be used as a viable measure of dynamical complexity in the ionosphere with portions showing
116 lower values of Tsallis entropy indicating lower dynamical complexity, with a good relationship
117 with Lyapunov exponents. They found a phase transition from higher dimension during quiet
118 days to Lower dimension during storm.

119

120 The low latitude region where Nigeria is situated is known as the equatorial anomaly region, this
121 region is known for equatorial ionization anomaly, which is due to the fountain effect. Off the

122 equator the E region electric field maps along the magnetic field up to the F-region altitude in the
123 low latitude, this eastward electric field (E) interacts with the magnetic field B at the F region
124 during the day. This results in the electrodynamic lifting of the F-region plasma over the equator,
125 known as EXB drift. The uplifted plasma over the equator moves along the magnetic line in
126 response to gravity, diffusion and pressure gradients and hence, the fountain effect. The fountain
127 effect being controlled by the EXB drift shows the dynamics of the diurnal variation equatorial
128 anomaly (Abdu, 1997; Unnikrishnan 2010). There is a reduction in the F region ionization
129 density at the magnetic equator and also much enhanced ionization density at the two anomaly
130 crests within $\pm 15^\circ$ of the magnetic latitude north and south of the equator (Rama Rao et al.,
131 2006). The equatorial ionization anomaly and other natural processes which includes various
132 ionization processes and recombination; influx of solar wind, photoionization processes and so
133 many other factors that occur due to variations in solar activities, have a great influence on the
134 systems of the ionosphere, due to their effects on internal dynamics of the ionosphere. This
135 portrays the ionosphere as a typical natural system with continuous interaction with its external
136 environment which led to the study of the influence of the sun on the ionosphere (Ogunsua et al.,
137 2014).

138 The ionosphere possesses a significant level of nonlinear variations that requires more
139 investigation which can be studied and characterized using nonlinear approach like the chaoticity
140 and dynamical complexity for the study of its dynamics. The need to study the daily variation in
141 the dynamical complexity of the ionosphere arises from the established knowledge and
142 understanding which shows that the ionosphere is a complex system with so many variations that
143 can arise from various dynamical changes that can be due to various changes in different
144 processes that contribute to the behavior and nature of the ionosphere. Rabiou et al., (2007)
145 affirmed that characterizing the ionosphere is of utmost importance due to the numerous
146 complexities associated with the region. The scale of these numerous complexities interestingly
147 changes at times from one day to another.

148 The concept of chaos as previously applied to ionospheric and magnetospheric studies on quiet
149 and stormy conditions are limited. Most investigations have been based on only quiet and storm
150 conditions for all studies carried out, and none of the previous works involved the use of quiet
151 and disturbed day classification of geophysical conditions until recently by Ogunsua et

152 al.,(2014), where we considered the comparative use of Lyapunov exponent and Tsallis entropy
153 as proxies for the internal dynamics of the ionosphere. This is the main reason for the
154 consideration of day to day variation of these parameters in this work.

155 **2.0 Data and Methodology**

156 The data used for this study is the global positioning system (GPS) total electron content (TEC)
157 data obtained from 5 GPS satellite receiver stations. Table 1 shows the coordinates of the
158 stations. These receivers take the measure of slant TEC within $1m^2$ columnar unit of the cross
159 section along the ray path of the satellite and the receiver which is given by

$$160 \text{ STEC} = \int_{\text{receiver}}^{\text{Satellite}} Ndl \quad (1)$$

161 The observation of the total number of free electron along the ray path are derived from the
162 frequency $L_1(1572.42 \text{ MHz})$ and $L_2(1227.60 \text{ MHz})$ of Global Positioning System(GPS), that
163 provide the relative ionosphere delay of electromagnetic waves travelling through the medium
164 (Saito et al.,1998). The Slant TEC is projected to vertical TEC using the thin shell model
165 assuming the height of 350m (Klobuchar,1986).

$$166 \text{ VTEC} = \text{STEC} \cdot \cos[\arcsin(R_e \cos\theta / R_e + h_{max})] \quad (2)$$

167 Where $R_e = 6378km$ (radius of the earth), $h_{max} = 350km$ (the vertical height assumed from
168 the satellite) and $\theta = \text{elevation angle at ground station}$

169

170 In this study, 5 GPS TEC measuring stations lying within the low latitude region were
171 considered, as shown in table 1. The TEC data obtained for January to December 2011 were
172 considered for this study and the data are given at 1min sampling time. The TEC data were
173 subjected to various analyses which will be discussed in the next section. The day to day
174 variations of the chaotic behavior and dynamical complexity were studied for the entire year.
175 The surrogate data tests for non linearity were also conducted for both the dynamical and
176 geometrical aspects.

177 **3.0 Methods of Data Analysis and Results**

178 3.1 Time series analysis

179 Time series can be seen as a numerical account that describes the state of a system, from which it
180 was measured. A given time series, S_n can be defined as a sequence of scalar measurement of a
181 particular quantity taken as series at different portion in time for a given time interval(Δt). The
182 time series describe the physical appearance of an entire system, as seen in Fig 1. However it
183 may not always describe the internal dynamics of that system. A system like the ionosphere
184 possesses a dominant dynamics that can be seen as diurnal so the data should be treated so as to
185 be able to see its internal dynamics. The measured TEC time series were plotted to see the
186 dynamics of the system. A typical plot of TEC usually has a dominant dynamics (see fig 1)
187 which may be seen as the diurnal behavior, however, it can also be seen that there is also a
188 presence of fluctuations (which appear to be nonlinear) in the system as a result of the internal
189 dynamics of the ionosphere and space plasma system, due to different activities in the
190 ionosphere. Therefore there is need to minimize the influence of the diurnal variations since we
191 are more interested in the nonlinear internal dynamics of the system in this study, to do so the
192 TEC time series was detrended by carrying out the following analysis below:

193 Since for the given daily data of 1minute sampling time there are 1440 data points per day. Then
194 there exists a time series t_i , where $i = 1,2,3 \dots 1440$ represents the observed time series, and
195 there also exists a set of u_i where $i = 1,2,3 \dots 1440$, such that the diurnal variation reduced time
196 is given by

$$197 \quad T_i = t_i - u_j \quad (3)$$

198 Where $i = 1,2,3, \dots, j = \text{mod}(i, 1440)$, if $\text{mod}(j, 1440) \neq 0$, and $j = 1440$ if $d(j, 1440) = 0$.
199 This method will give the detrended time series represented by T_i obtained from the original
200 TEC data as shown in fig 2. This method is similar to that used by (Unnikrishnan et al., 2006,
201 Unnikrishnan 2010), the further explanations on the dynamical results can be found in (Kumar et
202 al., 2004). The detrended time series were subjected to further analyses for the Phase space
203 reconstruction and also to obtain the values of Lyapunov exponents, correlation dimension,
204 Tsallis entropy and the implementation of surrogate data test.

205

206 3.1.1 Phase Space reconstruction and Non Linear Time Series Analysis

207 The study of chaoticity and dynamical complexity in a dynamical system requires a nonlinear
208 approach, due to the fact that systems described by these phenomena can be referred to as
209 nonlinear complex systems. The magnetosphere and the ionosphere are good examples of such
210 systems. To be able to study such phenomena some nonlinear time series analysis can be carried
211 out on the time series data describing such a system. The detrended time series of TEC
212 measurement is subjected to some nonlinear time series data analysis to obtain the mutual
213 information and false nearest neighbours, embedding dimension and delay coordinates for the
214 phase space reconstruction, and the evaluation of other chaotic quantifiers namely: Lyapunov
215 Exponents, Correlation dimension, recurrence analysis and Entropy.

216 The phase space reconstruction helps to reveal the multidirectional aspect of the system. The
217 phase space reconstruction is based on embedding theorem, such that the phase space is
218 reconstructed to show the multidimensional nature as follows:

$$219 \mathbf{Y}_n = (\mathbf{s}_{n-(m-1)\tau}, \mathbf{s}_{n-(m-2)\tau}, \dots, \mathbf{s}_{n-\tau}, \mathbf{s}_n) \quad (4)$$

220 where \mathbf{Y}_n are vector in phase space. The proper choice of embedding dimension (m) and delay
221 Time (τ) are essential for phase space reconstruction (Fraser and Swinney,1986; Kennel et
222 al.,1992) .

223 If the plot showing the time delayed mutual information shows a marked minimum that value
224 can be considered as a responsible time delay; Fig 3 shows the mutual information plotted
225 against time delay. Likewise, the minimal embedding dimension, which correspond to the
226 minimum number of the false nearest neighbours can be treated as the optimum value of
227 embedding dimension in (Unnikrishnan et al.,2006, Unnikrishnan, 2010). A plot of fraction of
228 false nearest neighbours against embedding dimension can be seen in Fig 4. It was observed that
229 for all the daily detrended TEC time series the choice of $\tau \geq 30$ and $m \geq 4$ values of delay and
230 embedding dimension above these values are suitable for analysis of data for all stations. The
231 choice of $\tau = 30$ and $m = 5$ were mostly used to analyze the dynamical aspects for all the
232 stations. The reconstructed Phase space trajectory is shown in Fig 5

233 3.1.2 Lyapunov Exponents

234 The Lyapunov exponent has been a very important quantifier for the determination of chaos in a
 235 dynamical system. This quantifier is also used for the determination of chaos in time series,
 236 representing natural systems like the ionosphere and magnetosphere (Unnikrishnan 2008, 2010).
 237 A positive Lyapunov exponent indicates divergence of trajectory in one dimension, or alternative
 238 an expansion of volume, which can also be said to indicate repulsion, or attraction from a fixed
 239 point. A positive Lyapunov exponent indicates that there is evidence of chaos in a dissipative
 240 deterministic system, where the positive Lyapunov exponent indicates divergence of trajectory in
 241 one direction or expansion of value and a negative value shows convergence at trajectory or
 242 contraction of volume along another direction.

243 The largest Lyapunov exponent (λ_1) can be used to determine the rate of divergence as indicated
 244 by (Wolf et al.,1985)

245 Where

$$246 \lambda_1 = \lim_{r \rightarrow \infty} \frac{1}{t} \ln \frac{\Delta x(t)}{x(0)} = \lim_{r \rightarrow \infty} \frac{1}{t} \sum_{i=1}^t \ln \left(\frac{\Delta x(t_i)}{\Delta x(t_{i-1})} \right) \quad (5)$$

247 The Lyapunov exponent was computed for the TEC values measured from Different stations.
 248 The evolution in state space was scanned with $\tau = 30$, $m = 5$, is shown in fig 6. The day to day
 249 variations of the Lyapunov exponent was computed for the entire year to so as to study the
 250 annual trend of variation. This was implemented using the method introduced by Rosenstein
 251 (1993), and Hegger et al., (1994), both algorithms use very similar methods. Lyapunov
 252 exponents were also computed for varying time delay at constant embedding dimension and also
 253 for varying embedding dimension, to check for the stability with changes in trajectory. These can
 254 be seen in fig. 6b and 6c. The day to day values of Lyapunov exponent plotted for the Enugu
 255 station and for Toro station are shown in fig 7a to 7b. The plots of the day to day values show the
 256 transient variation of the ionosphere and a wavelike yearly pattern.

257 **3.1.3 Correlation Dimension**

258 Another relevant method to study the underlying dynamics or internal dynamics of a system is to
 259 evaluate the dimension of the system. The correlation dimension gives a good approximation of
 260 this as suggested by Grassberger and Procaccia (1983a; b). The correlation dimension is

261 preferred over the box counting dimension because it takes into account the density of points on
 262 the attractor (Strogatz 1994). The correlation dimension D is defined as

$$263 \quad D = \lim_{r \rightarrow 0} \frac{\ln C(r)}{\ln r} \quad (6)$$

264 The term $C(r)$ is the correlation sum for radius (r) where for a small radius (r) the correlation
 265 sum can be seen as $C(r) \sim r^d$ for $r \rightarrow 0$. The correlation sum is dependent of the embedding
 266 dimension (m) of the reconstructed phase space and it is also dependent of the length of the time
 267 series N as follows

$$268 \quad C(r) = \frac{2}{N(N-1)} \sum_{i=1}^N \sum_{j=i+1}^N \Theta(r - \|y_i - y_j\|) \quad (7)$$

269 Where Θ is the Heaviside step function, with $\Theta(H) = 0$ if $H \leq 0$ and $\Theta(H) = 1$ for $H > 0$.

270 The correlation dimension was computed using the Theiler algorithm approach, with Theiler
 271 window (w) at 180. The Theiler window was chosen to be approximately equal to the product of
 272 m and τ . A similar approach to the computation of correlation dimension was used by
 273 Unnikrishnan and Ravindran (2010) to determine the correlation dimension of detrended TEC
 274 data for some stations in India which lies within the equatorial region, like Nigeria. Ogunsua et
 275 al., (2014) also used similar methods for some detrended TEC from Nigerian stations.

276 The correlation dimension for data taken for the quietest day of October 2011 and the most
 277 disturbed day of October 2011 from Birnin Kebbi GPS TEC measuring station were represented
 278 by Fig 8a and Fig 8b respectively. The correlation dimension saturates at $m \geq 4$ for the quietest
 279 day of the month and at $m \geq 5$ for the most disturbed day. In this illustration the most disturbed
 280 day of this month fall within the storm period of October 2011. The classification of days into
 281 quiet and disturbed days in the month of October 2011 enables us to compare the quiet and storm
 282 periods together while comparing the quiet days with some relatively disturbed days.

283 **3.1.4 Computation of Tsallis Entropy and Principles of Nonextensive Tsallis Entropy**

284 Entropy measures are very important statistical techniques that can be used to describe the
 285 dynamical nature of a system. The Tsallis entropy can be used to describe the dynamical
 286 complexity of a system and to also understand the nonlinear dynamics like chaos which may

287 exist in a natural system. The use of entropy measure as a method to describe the state of a
 288 physical system has been employed into information theory for decades. The computation of
 289 entropy allows us to describe the state of disorderliness in a system, one can generalize this same
 290 concept to characterize the amount of information stored in more general probability
 291 distributions (Kantz & Shrieber 2003, Balasis et al.,2009). The concept of information theory is
 292 basically concerned with these principles. The information theory gives us an important
 293 approach to time series analysis. If our time series which is a stream of numbers, is given as a
 294 source of information such that this numbers are distributed according to some probability
 295 distribution, and transitions between numbers occur with well-defined probabilities. One can
 296 deduce same average behaviour of the system at a different point and for the future. The term
 297 entropy is used in both physics and information theory to describe the amount of uncertainty or
 298 information inherent in an object or system (Kantz and schrieber 2003). The state of an open
 299 system is usually associated with a degree of uncertainty that can be quantified by the
 300 Boltzmann-Gibbs entropy, a very useful uncertainty measure in statistical mechanics. However
 301 Boltzmann-Gibbs entropy cannot, describe non-equilibrium physical systems with large
 302 variability and multifractal structure such as the solar wind (Burgala et al., 2007, Balasis et al.,
 303 2008). One of the crucial properties of the Boltzmann-Gibbs entropy in the context of classical
 304 thermodynamics is extensivity, namely proportionality with the number of elements of the
 305 system. The Boltzmann-Gibbs entropy satisfies this prescription if the subsystems are
 306 statistically (quasi-) independent, or typically if the correlations within the system are essentially
 307 local. In such cases the system is called extensive. In general however, the situation is not of this
 308 type and correlations may be far from negligible at all scales. In such cases, the Boltzmann-
 309 Gibbs entropy is nonextensive (Balasis et. al., 2008, 2009). These generalizations above were
 310 proposed by Tsallis (1988), who was inspired by the probabilistic description of multifractal
 311 geometries. Tsallis (1988, 1998) introduced an entropy measure by presenting an entropic
 312 expression characterized by an index q which leads to a nonextensive statistics,

$$313 \quad S_q = k \frac{1}{q-1} \left(1 - \sum_{i=1}^W p_i^q \right) \quad (8)$$

314 Where p_i are the probabilities associated with the microscopic configurations, W is their total
 315 number, q is a real number, and k is Boltzmann's constant. The value q is a measure of the
 316 nonextensivity of the system: $q \rightarrow 1$ corresponds to the standard extensive Boltzmann-Gibbs

317 statistics. This is the basis of the so called nonextensive statistical mechanics, which generalizes
 318 the Boltzmann-Gibbs theory. The entropic index q characterizes the degree of nonadditivity
 319 reflected in the following pseudoadditivity rule:

$$320 \quad \frac{S_q(A+B)}{k} = \left[\frac{S_q(A)}{k} \right] + \left[\frac{S_q(B)}{k} \right] + (1 - q)[S_q(A)/k] \left[\frac{S_q(B)}{k} \right]. \quad (9)$$

321 The cases $q > 1$ and $q < 1$, correspond to subadditivity (or subextensivity) and superadditivity
 322 (or superextensivity), respectively and $q = 1$ represents additivity (or extensivity). For
 323 subsystems that have special theory probability correlations, extensivity is not a valid for
 324 Boltzmann-Gibbs entropy in such cases, but may occur for S_q with a particular value of the index
 325 q . Such systems are sometimes referred to as nonextensive (Boon and Tsallis, 2005, Balasis et al
 326 2008, 2009). The parameter q itself is not a measure of the complexity of the system, but
 327 measures the degree of nonextensivity of the system. It is the time variations of the Tsallis
 328 entropy for a given $q(S_q)$ that quantify the dynamic changes of the complexity of the system.
 329 Lower S_q values characterize the portions of the signal with lower complexity. In this
 330 presentation we estimate S_q on the basis of the concept of symbolic dynamics and by using the
 331 technique of lumping (Balasis et al. 2008, 2009).

332 A comparison of Tsallis entropy with Lyapunov exponents computed for the same set of data has
 333 been carried out in this work, to see the efficacy of the combined usage of both parameters. This
 334 is based on the established facts that variations in the values of Tsallis entropy can be linked with
 335 that of Lyapunov exponents chaotic behavior in systems as seen in (Baranger et al., 2012;
 336 Anastasiadis et al., 2005; Kalogeropoulos et al., 2012;2013). Coraddu et al., (2005) showed the
 337 Tsallis entropy generalization for Lyapunov exponents. Further details can be found in Ogunsua
 338 et al., (2014),

339 they were able to investigate the similarities in their response to the complex dynamics of the
 340 ionosphere, and this informs the further use of the two quantities as indices to study the day to
 341 day variation of ionospheric behaviour in this work.

342 The values of these entropy measures were also computed in order to study the dynamical
 343 complexity of the system under observation (the ionosphere). The day to day values of Tsallis

344 entropy were computed for the entire year for different stations. The day to day values of Tsallis
345 entropy plotted for the Enugu station and for Toro station are shown in fig 9(a and b). The plots
346 of the day to day values show the transient variation of the ionosphere and a wavelike yearly
347 pattern.

348 **3.2 Non linearity Test using surrogate data**

349 The test for non-linearity using the method of surrogate data according to Kantz and Schreiber
350 (2003) has proven to be a good test for non-linearity in time series describing a system. It has
351 been accepted that the method of surrogate data test could be a successful tool for the
352 identification of nonlinear deterministic structure in an experimental data (Pavlos et al., 1999).
353 This method involves creating a test of significance of difference between linearly developed
354 surrogate and original nonlinear time series to be tested. The test is done by carrying out the
355 computation of the same quantity on both surrogates and the original time series and then
356 checking for the significance of difference between the results obtained from the surrogates with
357 the original data. Theiler et al (1992) suggested the creation of surrogate data by using Monte
358 Carlo techniques for accurate results. According to this method, typical characteristic of data
359 under study are compared with those of stochastic signals (surrogates), which have the same
360 auto-correlation function and the power spectrum of the original time series. It can be safely
361 concluded from the test of significance carried out on the surrogate and the original data that, a
362 stationary linear Gaussian Stochastic model cannot describe the process under study provided
363 that the behaviour of the original data and the surrogate data are significantly different.

364
365 In this work 10 surrogate data were generated from the original data set. The geometrical and
366 dynamical characteristics of the original data were then compared to that of the surrogates using
367 the statistical method of significance of difference which can be defined as

$$368 \quad S = \frac{\alpha_{Surr} - \alpha_{Original}}{\sigma} \quad (13)$$

370
371 Where α_{Surr} is the mean value of the computed quantity for the surrogate data and $\alpha_{Original}$ is
372 the same quantity computed for the original TEC data, σ is the standard deviation of the same

373 quantity computed for the surrogate data. The significance of difference considered for the null
374 hypothesis to be rejected here is greater than 2, which enables us to be able to reject the null
375 hypothesis that the original TEC data describing the ionospheric system can be modeled using a
376 Gaussian linear stochastic model with confidence greater than 95%.

377 The surrogate data test for all stations used in this study show that the Lyapunov exponent of
378 the surrogate data for the selected days in October are shown in the Table below The results
379 show that the surrogate data test for Lyapunov exponent show a significance of difference
380 greater than 2 for all the selected days for all the stations. Similar results were obtained for
381 Mutual Information, Fraction of False Nearest Neighbours and Correlation Dimension. This
382 result gives us the confidence to reject the null hypothesis that the data used cannot be modeled
383 using a linear Gaussian stochastic model, which shows that the system is a nonlinear system with
384 some level of determinism. Fig. 10 shows the plots comparing the mutual information plotted
385 against time delay for the original detrended data blue with the mutual information for the
386 surrogate data for TEC data measured at Lagos for the quietest day of March 2011, while Fig. 11
387 is comparing fraction of false nearest neighbours for the same set of data. Tables 2a shows the
388 values of Lyapunov exponents for both original detrended and its surrogate data for TEC
389 measured in Lagos during the quietest days and Table 2b shows the values of Lyapunov
390 exponents for both original detrended and its surrogate data for TEC measured in Lagos during
391 the most disturbed days of October 2011. The result obtained from the surrogate data test shows
392 that we cannot represent the original detrended data with a linear Gaussian stochastic model.

393

394 **3.3 Trend filtering using the moving average approach for the daily Values**

395 The trend of a fluctuating time series can be made clearer to reveal the general pattern of that
396 time series, and to make the fluctuating pattern of the daily variation of the chaoticity and
397 dynamical complexity measures clearer in the work, the moving average method has been
398 employed. The method of moving average filtering has found its applications geophysics (e.g.
399 Bloomfield 1992; Bloomfield and Nychka 1992; Baillie and Chung 2002), and in other areas like
400 financial time series analysis, microeconomics, biological sciences and medical sciences. The
401 various fields mentioned require different trend filtering method depending on the structure of

402 the time series to be analyzed. Different filtering processes that can be used to reveal the trend
 403 includes the moving average filters, exponential filters, band-pass filtering, median filtering etc.

404 Suppose we have a time series $z[t]$ such that $t = 1, 2, 3 \dots \dots n$, where 'n' could assume any
 405 value. If $z[t]$ consists of a consistent varying trend component that appears over a longer period
 406 of time t given as $u[t]$ and a more rapidly varying component $v[t]$. The goal of trend filtering in
 407 any research is to estimate either of the two components (Kim et al., 2009). The purpose of trend
 408 filtering in this work is to further reveal the general slow varying trend that appears to be obvious
 409 in the daily variation of the values of the chaoticity and dynamical complexity of the ionosphere,
 410 which might appear to be obviously varying with the yearly solar activity (a quantity with slow
 411 varying trend). To make $u[t]$ which represents the general slow varying trend smoother and in
 412 the process reduce $v[t]$ we apply the moving average filter.

413 If we assume $z[t]$ to be our time series representing the daily variation of the values of the
 414 chaoticity and dynamical complexity of the ionosphere, then our smoothing with weighting
 415 vector/filter w_j will create the new sequence u_j as

$$416 \quad u[t] = z[t] * w[n] = \frac{1}{2k+1} \sum_{i=-k}^k x[n-1]. \quad (14)$$

417 In this work the Savitzky-Golay method of smoothing proposed by Savitzky and Goley (1967),
 418 which is a generalized form of moving average was applied to the trend smoothing of the daily
 419 variation of the chaoticity and dynamical complexity of the ionosphere. In this case it performs a
 420 least square fit to a small set of $L(= 2k + 1)$ consecutive data to a polynomial and then takes
 421 midpoint of the polynomial curve as output. The smoothed time series in this work will now be
 422 given as

$$423 \quad u[t] = z[t] * \omega[n] = \frac{\sum_{i=-k}^k A_i * x[n-1]}{\sum_{i=-k}^k A_i} \quad (15)$$

424 where, $\omega[n] = \frac{A_n}{\sum_{i=-k}^k A_i}$, $-k \leq n \leq k$ such that A_i controls the order of polynomial. A similar
 425 method was described in Reddy et al., (2010).

426 The smoothed daily variation and the original data and the plot of the smoothed variation only,
 427 for the Lyapunov exponents of the detrended TEC measured at the Enugu and Toro are shown in

428 fig 12(a and b). The smoothed day to day variation for Tsallis entropy for the detrended TEC
429 measured at Enugu and Toro stations respectively are shown in fig 13(a and b).

430 **4.0 DISCUSSION**

431 The results presented in the work reveals the dynamical characteristics of the ionosphere. These
432 characteristics are being discussed in this section, considering the time series treatment and phase
433 space reconstruction; the study of chaos using chaotic quantifiers and the use and comparison of
434 dynamical complexity measures in terms of their response to the variations on ionospheric
435 dynamics. Also being discussed, is the implication of the nonlinearity test using the surrogate
436 data and the comparison of the two quantifiers and their viability as indices for the continuous
437 study and characterization of the ionosphere

438
439 The time series analysis shows the appearance of some degree of nonlinearity in the internal
440 dynamics of the ionosphere. The time series plot in Fig. 1 shows the rise in TEC to peak at the
441 sunlit hours of the day, however it can be seen that the rising to the peak exhibited by the
442 ionosphere, which is the dominant dynamics during the day, make it impossible to clearly see the
443 internal dynamics of the system from the TEC time series plot. It can be seen that the TEC time
444 series curve is not a smooth curve with tiny variations, which probably describes a part of the
445 internal dynamics. These visible tiny variations around the edges of the time series plot can be
446 regarded as rate of change of TEC which is a phenomenon that can describe the influence of
447 scintillations in the ionosphere these variations are however more obvious during the night time
448 between 1100th and 1440th minutes of the day (that is, between about 1800 and 2400 hours of
449 the day). It should be noted here that scintillations has been described as a night time phenomena
450 associated with spread-F, and it occurs around pre-midnight and post-midnight periods (Vyas
451 and Chandra 1994; Vyas and Dayanandan 2011; Mukherjee et al.,2012; Bhattacharyya and
452 Pandit 2014). The detrended data shows the internal dynamics of the system more clearly, with a
453 pattern similar to the values around night period mentioned earlier. The post-sunset values
454 (especially at night time) in Fig.1 show a pattern similar pattern with the detrended TEC plot in
455 Fig 2. It has been established that TEC does not decrease totally throughout the night as expected
456 normally through simple theory that TEC builds up during the day, but it shows some anomalous
457 enhancements and variations and this can occur under a wide range of geophysical conditions

458 (Balan and Rao, 1987; Balan et al., 1991; Unnikrishnan and Ravindran, 2010). The delay
459 representation of the phase space reconstruction shows a trajectory that is clustered around its
460 origin, for all the stations, which can be seen as an indication of the possible presence of chaos.
461 The degree of closeness of these trajectories however varies for different days from one station
462 to another, resulting from varying degrees of variations in stochasticity and determinism. The
463 varying degrees of variations in stochasticity and determinism can be attributed to the daily
464 variations and local time variations of photoionization, recombination, influx of solar wind and
465 other factors that may influence the daily variations of TEC (Unnikrishnan 2010).

466
467 The positive values of Lyapunov exponent indicate the presence of chaos (Wolf et al., 1985;
468 Rosenstein et al., 1993; Hegger et al., 1999; Kantz and Schreiber, 2003). The presence of chaos
469 was revealed by the positive Lyapunov exponent computed from all stations and this as a result
470 of the fact that the ionosphere is a system controlled by many parameters influencing its internal
471 dynamics. Because of its extreme sensitivity to solar activity, the ionosphere is a very sensitive
472 monitor of solar events. The ionospheric structure and peak densities in the ionosphere vary
473 greatly with time (sunspot cycle, seasonally and diurnally), with geographical location (polar,
474 auroral zones, mild-latitudes, and equatorial regions), and with certain solar-related ionospheric
475 disturbances. During and following a geomagnetic storm, the ionospheric changes around the
476 globe, as observed from ground site can appear chaotic (Fuller-Rowell et al., 1994; Cosolini and
477 Chang, 2001; Unnikrishnan and Ravindran, 2010). The recorded presence of chaos as indicated
478 by the positive values of Lyapunov exponent was found in all the computations, for all the TEC
479 values obtained for the selected days from all the measuring stations used in this work. This can
480 be expected as it agrees with results from previous works that show that there is a reasonable
481 presence of chaos in the ionosphere, even in the midst of the influence of stochastic drivers like
482 solar wind (Bhattacharyya, 1990; Wernik and Yeh, 1994; Kumar et al., 2004; Unnikrishnan et
483 al., 2006a,b; Unnikrishnan, 2010). However the values of Lyapunov exponents vary from day to
484 day due to variations in ionospheric processes for different days on the same latitude as seen in
485 Fig. 7(a and b) with Fig. 12(a and b) showing the day to day variation (upper panel) and the
486 smoothed curve of the day to day variation (lower panel) for the entire year. There are also
487 latitudinal variations due to spatial variations in the various ionospheric processes taking place

488 simultaneously. The ionosphere is said to have a complex structure due to these varying
489 ionospheric processes.

490 The higher values of Lyapunov exponent during months of low solar activity (the solstices) is an
491 evidence that that the rate of exponential growth in infinitesimal perturbations in the ionosphere
492 leading to chaotic dynamics might be of higher degree during most of the days of those months
493 compared to days of the months with high solar activities showing lower values of Lyapunov
494 exponents (Unnikrishnan 2010, Unnikrishnan and Ravindran, 2010).

495
496 The results of the correlation dimension values computed are within the range of 2.7 to 3.2 with
497 the lower values occurring mostly during the storm periods. The lower dimension during the
498 storm periods compared to the quiet days may be due to the effect of a stochastic drivers like
499 strong solar wind and solar flares, that occurs during geomagnetic storms on the internal
500 dynamics of the ionosphere, this could have been as a result of the fact that the internal dynamics
501 must have been suppressed by the external influence. The restructuring of the internal dynamics
502 of the ionosphere might be responsible for low dimension chaos during storm and also the lower
503 values of other measures like the Lyapunov exponents. The relatively disturbed day however
504 might have a higher dimension so long as it is not a storm period, and sometimes a relatively
505 disturbed day of the month might be a day with storm and in this case there is usually a lower
506 value of chaoticity and sometimes lower values of correlation dimension as well. The lower
507 value of chaoticity and dimension in ionosphere during storms indicates a phase transition from
508 higher values during the quiet periods to lower values during storm periods which may be due to
509 the modification of the ionosphere by the influx of high intensity solar wind during the storm
510 period (Unnikrishnan et al., 2006a, b; Unnikrishnan 2010; Unnikrishnan and Ravindran, 2010).

511
512 The surrogate data test shows significance of difference greater than 2 for all the computed
513 measures which enables rejection of the null hypothesis that the ionospheric system can be
514 represented with a linear model for all the data used from the stations. However it was
515 discovered that the lower significance of difference corresponds to the lower values of Lyapunov
516 exponents during storm and extremely disturbed periods (see tables 2a and 2b). This may be due
517 the rise in stochasticity during the storm period as a result of drop in values of computed
518 quantities like Lyapunov exponents. Our ability to reject the Null hypothesis for all stations

519 however shows the presence of determinism and confirms that the underlying dynamics of the
520 ionosphere is mostly non-linear. This further validates the presence of chaos since the surrogate
521 data test for non-linearity show that out detrended TEC is not a Gaussian (linear) stochastic
522 signal (Unnikrishnan 2010). However for some of the data sets the saturation of the average
523 mutual information observed at delay close to unity (as seen in fig. 3) and the saturation
524 Lyapunov exponent in the first time step (Fig. 6) indicate that there could be a high influence of
525 stochasticity in the system.

526
527

528 The Tsallis entropy was able to show the deterministic behavior of the ionosphere considering
529 its response during storm periods compared to other relatively quiet periods as the rapid drop in
530 values of Tsallis entropy during storm show that there is a transition from higher complexity
531 during quiet period to lower complexity during storms, this response in the values of Tsallis
532 entropy is similar to the response of Lyapunov exponent values during storm. This reaction to
533 storm shown by the values of Tsallis entropy computed for TEC was also described by the
534 reaction of Tsallis entropy computed for Dst during storm periods (Balasis et al., 2008, 2009). A
535 closer observation of the day-to-day variability within a month shows that the values were much
536 lower for storm periods compared to the nearest relative quiet period. For example, the storm
537 that occurred on the 25th of October resulted in lower values of Lyapunov exponent and Tsallis
538 entropy compared to relatively quiet days close to it. The reaction to storm may be due to the
539 influence of stochastic driver like strong solar wind flowing into the system as a result of solar
540 flare or CMEs that produces the geomagnetic storms. Although there is always an influence of
541 corpuscular radiation in form of solar wind flowing from the sun into the ionosphere, the
542 influence is usually low for days without storm compared to days with geomagnetic storms as a
543 result of solar flares, CMEs etc (Unnikrishnan et al., 2006a,b; Unnikrishnan, 2010, Ogunsua et al
544 2014).

545

546 The presence of chaos and high variations in the dynamical complexity, even at quiet periods in
547 the ionosphere may be due to the internal dynamics and inherent irregularities of the ionosphere
548 which exhibit non-linear properties. However, this inherent dynamics may be complicated by
549 external factors like Geomagnetic storms. This may be the main reason for the drop in the values

550 of Lyapunov exponent and Tsallis entropy during storms. According to Unnikrishnan et al.,
551 (2006a,b), geomagnetic storms are extreme forms of space weather, during which external
552 driving forces , mainly due to solar wind, subsequent plasmasphere -ionosphere coupling, and
553 related disturbed electric field and wind patterns will develop. This in turn creates many active
554 degrees of freedom with various levels of coupling among them, which alters and modifies the
555 quiet time states of ionosphere, during a storm period. This new situation developed by a storm,
556 may modify the stability/instability conditions of ionosphere, due to the superposition of various
557 active degrees of freedom.

558

559 The observation from the day-to-day variability of Lyapunov exponent and Tsallis entropy also
560 show irregular pattern for all stations. These irregular variations might be due to the same factors
561 mentioned before (i.e internal irregularities due to so many factors described and also due to
562 variation in the influx of the external stochastic drivers). The day-to-day variability for the entire
563 year shows a “wavelike” pattern with the values dropping to lower values during the equinox
564 months especially during March-April equinox. This can be seen as a form of semiannual
565 variation, possibly resulting from the higher energy inputs during equinoxes. This is because
566 solar wind is maximized at the equinoxes which might result in higher energy input that will
567 eventually suppress the internal dynamics to give lower values of chaoticity. The modification of
568 the ionosphere as a result of the higher energy input resulting from the maximized influx of solar
569 wind has been reported to be responsible for the lower values of chaoticity when averaged
570 compared to the days of the year with lower solar wind inputs as reported by Unnikrishnan et al.,
571 2006; 2010; Ogunsua et al., 2014. The semiannual pattern has been found to be similar for
572 different stations as seen in Figs. 7 & 12 and Figs. 9 & 13 for Lyapunov exponents and Tsallis
573 entropy respectively. Figs.9 and 13 show the smoothed curves for Lyapunov exponent and
574 Tsallis entropy respectively, with the drop in values at equinoxes showing more clearly. The
575 phase transition in chaoticity and dynamical complexity is also responsible for the wavelike
576 variations, with values of Lyapunov exponent and Tsallis entropy dropping during the equinoxial
577 months, and this may be due to the influence of the daily influx of the solar wind having higher
578 values during equinoxes due to the proximity of the Earth to the sun during this period compared
579 to the solstice months.

580

581 The wavelike pattern observed has been described to be as a result of self organized critical
582 (SOC) phenomenon, a phenomenon which has been found to exist in both the magnetosphere
583 and the ionosphere or the space plasma system in general, due to coupling between the two
584 systems, since the magnetosphere couples the ionosphere tightly to the solar wind (Lui, 2002).
585 Many literatures has shown the existence of chaos in the SOC in the magnetosphere (chang et
586 al.,1992,1998,1999; Consolini et al., 1996 Chapman et al., 1998; Freeman and Watkins 2002
587 and; Koselov and Koselova, 2001. Uritsky et al., (2003) and; Chang et al., (1992). The existence
588 of SOC in space plasma system involving both the ionosphere the the magnetosphere was
589 described by (Lui, 2002; Chang et al., 2002; Chang et al., 2004)

590

591 The variation along the latitude also shows the inconsistence and complexity of the ionospheric
592 processes. This is the reason why for the same day of the month the values of Lyapunov
593 exponent vary from one station to another. Lyapunov exponent however, appears to respond
594 better to changes in solar activities compared to Tsallis entropy with more distinct results. This
595 may be due to the fact that Tsallis entropy being not only a measure of complexity, but also a
596 measure of disorderliness in a system might not be as perfect in describing chaos as Lyapunov
597 exponent. Kalogeropoulos (2009) and Baranger et.al (2002) observed that Tsallis entropy has a
598 relationship that is not totally linear in all cases at different level of chaos with Lyapunov
599 exponent as a measure of chaos.

600

601 There are also many variations in the internal dynamics of the ionosphere that could lead to
602 changes in chaotic behavior. The variations of Lyapunov exponents during quiet days might be
603 as a result of different variations in the intrinsic dynamics of the ionosphere. Difference in
604 variation pattern at different stations for the same quiet day might also be due to the same reason.
605 It can be affirmed that the ionosphere is a complex system that varies with a short latitudinal or
606 longitudinal interval such that even stations with one or two degrees of latitudinal differences
607 might record different values on the same day for both quiet and disturbed periods and that the
608 same might also occur for storm periods. This is illustrated by the different pattern of variation of
609 TEC recorded from different stations within such a close range as used in this study.

610

611 These Latitudinal variation in the values of Lyapunov exponents and Tsallis entropy can be
612 further described by the behavior of the TEC because there can be a more sporadic rate of
613 change in TEC as seen in the time series plots as a result of irregularities in the internal dynamics
614 of the ionosphere, which might be as a result of plasma bubbles. Irregularities develop in the
615 evening hours at F region altitudes of magnetic equator, in the form of depletions, frequently
616 referred to as bubbles. The edges of these depletions are very sharp resulting in large time rate of
617 TEC in the equatorial ionosphere, even during magnetically quiet conditions. The large gradient
618 of the equatorial ionization persists in the local post-sunset hours till about 2100 h LT.
619 (DasGupta et al., 2007; Unnikrishnan and Ravindran, 2010). The TEC data for one station might
620 experience an extremely sharp rate of change in TEC that may be due to some plasma bubbles in
621 that region while the TEC from the other station stays normal. These variations in the various
622 internal dynamics like plasma bubbles leading to scintillation can cause variations in the
623 dynamical response of the TEC. Hence, the irregular variation in the values of the Lyapunov
624 exponent and Tsallis entropy even in quiet periods for two relatively close stations may be due to
625 these irregularities. This might also be responsible for the quiet days in the same station having
626 lower values of Lyapunov exponent compared to higher values recorded for disturbed days
627 without the external influence of storms.

628
629 The variations of these chaos and dynamical complexity parameters might also be as a result of
630 the anomalous TEC enhancements that might occur at nights (Balan and Rao (1987); Balan et
631 al., 1991). These effects can also be seen more clearly in the Tsallis entropy values for the five
632 period window for quiet day of January, 2011, because the night time value is higher and it also
633 show a much higher series of fluctuations during this period compared to other periods. As
634 mentioned in Unnikrishnan and Ravindran (2010), the irregular changes in the dynamical
635 characteristics of TEC from the results of Lyapunov exponent and Tsallis entropy also may be
636 due to the collisional Raleigh-Taylor instability which may give rise to a few large irregularities
637 in L band measurements (Rama Rao et al., 2006; Sripathi et al., 2008) all these can be seen as
638 internal factors responsible for variations in the dynamical response of TEC as recorded from the
639 values of the Lyapunov exponents and Tsallis entropy completed for days without storm which
640 might be quiet or disturbed according to classification and also could account for higher values

641 of these qualifiers during disturbed days compared quiet days. During storms however, the
642 values were much lower

643
644 Earlier we, (Ogunsua et al., 2014) showed the appearance and variation of chaoticity quiet and
645 disturbed day classification by international most quiet day (IQD) and internal most disturbed
646 day (IDD) classification, as compared to quiet and storm period used by Unnikrishnan (2006;
647 2010). We were able establish that a relatively quiet day may be less chaotic compared to a
648 relatively disturbed day unlike the result presented by Unnikrishnan (2006; 2010) for quiet and
649 storm period. Also the combined use of both Lyapunov exponent and Tsallis entropy for the first
650 time was found to have a high correlation mostly above 80%, which has stimulated the interest
651 for further research using the two diagnosis for the study of ionospheric dynamics.

652
653 This work on the other hand presents the results for day to day variation and has revealed a
654 seasonal trend for both Lyapunov exponents and Tsallis entropy, which appear in wavelike in
655 form, with troughs during the two equinoxes. This was established for different stations used in
656 this research work. The results show the appearance of seasonal trend in spite of the sporadic
657 daily variation resulting from various changes in the internal dynamics. The seasonal trend has
658 provided another possible evidence of higher energy input during equinoxes, since it reveals the
659 effect of the annual energy input to the ionosphere. The day to day response these parameters has
660 also revealed the variations in the underlying dynamics of the system.

661
662 As a similarity between the present work and Ogunsua et al. (2014) the relationship between
663 Lyapunov exponent and Tsallis entropy can also be seen from this work, as the two quantifiers
664 exhibit similarities in their response to the dynamical behavior of the ionosphere with phase
665 transition at the same periods of time for all stations. A further investigation of this relationship
666 shows that all the daily values of Tsallis entropy correlates positively with the values of
667 Lyapunov exponent at values between 0.78 and 0.83.

668
669 The ability of these quantifiers to clearly reveal the ionospheric dynamical response to solar
670 activities and changes in its internal dynamics due to other factors is a valid proof of the

671 authenticity of the use of these chaotic and dynamical measures, as indices for ionospheric
672 studies.

673 **5.0 Conclusion**

674 The chaotic behaviour and dynamical complexity of low latitude ionosphere over some parts of
675 Nigeria was investigated using TEC time series measured Simultaneously at five different
676 stations namely Birnin Kebbi (geographic coordinates $12^{\circ}32'N$, $4^{\circ}12'E$; dip latitude $0.62^{\circ}N$),
677 Torro (geographic coordinates $10^{\circ}03'N$, $9^{\circ}04'E$; dip latitude $-0.82^{\circ}N$), Enugu (geographic
678 coordinates $6^{\circ}26'N$, $7^{\circ}30'E$; dip latitude $-3.21^{\circ}N$), Lagos (geographic coordinates $6^{\circ}27'N$,
679 $3^{\circ}23'E$; dip latitude $-3.07^{\circ}N$) and Yola (geographic coordinates $9^{\circ}12'N$, $12^{\circ}30'E$; dip
680 latitude $-1.39^{\circ}N$) within the low latitude region. The detrended TEC time series data obtained
681 from the GPS data measurement were analysed using different chaoticity and dynamical
682 complexity parameters.

683 The evidence of the presence of chaos in all the time series data was obtained for all the data
684 used, as indicated by the positive Lyapunov exponent. The results of Tsallis entropy show the
685 variations in the dynamical complexity of the ionosphere, which may be due to geomagnetic
686 storms and other phenomena like changes in the internal irregularities of the ionosphere. The
687 response of the Tsallis entropy to various changes in the ionosphere also shows the deterministic
688 nature of the system. The results of the Tsallis entropy show a lot of similarities with that of the
689 Lyapunov exponents between 0.78 and 0.81, with both results showing a phase transition from
690 higher values in the solstices to lower values during the equinoxial months. The values of
691 Lyapunov exponent were found lower for the days of the months in which storm was recorded
692 relative to the nearest relatively quiet days which agree with previous works by other
693 investigators. A similar pattern of results was obtained for the computed values of Tsallis
694 entropy. The random variations in the values of chaoticity in the detrended TEC describing the
695 internal dynamics of the ionosphere as seen in the result obtained from both Lyapunov exponent
696 and Tsallis entropy depicts the ionosphere as a system with a continuously changing internal
697 dynamics, which shows that the ionosphere is not totally deterministic but also has some
698 elements of stochasticity influencing its dynamical behaviour.

699

700 The phase transition in the systems of the ionosphere resulting in the lower values of the
701 chaoticity and dynamical complexity quantifiers during the geomagnetic storms and the
702 equinoxial months is the evidence that the ionosphere can be greatly modified by stochastic
703 drivers like solar wind and other incoming particle systems. The drop in values during equinoxes
704 can be seen as form of semiannual variation, a phenomenon peculiar to the low latitude regions.

705

706 Although the knowledge of being able to characterize the ionospheric behaviour using the two
707 major quantifiers shows their ability to measure level of determinism when used together, the
708 relationship between these two quantifiers calls for more research, in the use of these qualifiers,
709 to enable proper description and characterization of the state of ionosphere. The response of both
710 Tsallis entropy and Lyapunov exponents to changes in the ionosphere shows that the two
711 quantifiers can be used as indices to describe the processes/dynamics of the ionosphere.

712

713

714

715

716

717

718

719

720

721

722

723

724

725 **Acknowledgement**

726 The authors appreciate the editorial team and the referees for their contributions which have led
727 to the final shape of this paper. The GPS data used for this research were obtained from the public
728 archives of the Office of the Surveyor General of the Federation (OSGoF) of the Federal
729 Government of Nigeria, which is the mapping agency of Nigeria.

730

731

732

733

734

735

736

737

738

739

740

741

742

743

744

745

746

747 **References**

- 748 Abdu M.A.: Major Phenomena of the equatorial ionosphere thermosphere system under
749 disturbed conditions, *J.Atmos.Solten Physics.*,59(13), 1505 – 1519, 1997.
- 750 Anastasiadis, A.; Costa, L.; Gonzáles, C.; Honey, C.; Széliga, M. & Terhesiu, D. "Measures of
751 Structural Complexity in Networks", *Complex Systems Summer School 2005, Santa Fe. (2005).*
- 752 Bak, P., C. Tang, and K. Wiesenfeld, Self-Organized Criticality-an Explanation of 1/F Noise,
753 *Phys. Rev. Lett.*, 59(4), 381– 384, 1987.
- 754 Balan N., Rao,P.B.: Latitudinal variations of nighttime enhancements in total electron content,
755 *journal of Geophysical Research* 92 (A4), 3436 – 3440. 1987
- 756 Balan N., Bailey G.J., Balachandian. Nouv R.: Solar and Magnetic effects on the latitudinal
757 variations of nighttime TEC enhancement, *Annales Geophysicae* 9, 60 – 69. 1991
- 758 Balasis, G., and Manda M.: Can electromagnetic disturbances related to the recent great
759 earthquakes be detected by satellite magnetometers? *Tectonophysis* – 431, doi:
760 10.1016/j.texto.2006.05.038. 2007
- 761 Balasis, G., Daglis I.A., Papadimitrou, C., Kalimeri, M., Anastasiadis, A., Eftaxias, K.:
762 Dynamical complexity in D_{st} time series using non-extensive Tsallis entropy. *Geophysical*
763 *Research Letters* 35, L14102, doi:10.1029/2008GL034743. 2008
- 764 Balasis, G., Daglis I.A., Papadimitrou, C., Kalimeri, M., Anastasiadis, A., Eftaxias, K.:
765 Investigating Dynamical complexity in the magnetosphere using various entropy measures.
766 *Journal of Geophysical Research* 114, A00D06, doi:10.1029/2008JA014035. 2009
- 767 Ballie R. Chung S.: Modeling and forecasting from trend stationary long memory models, with
768 applications in climatology. *International journal of forecasting*, 18(2)215-226,2002.
- 769 Bhattacharyya, A: Chaotic behavior of ionosphere turbulence from scintillation measurements, *J.*
770 *Geophys. Res*, 17, 733 – 738, 1990.

771 Bhattacharyya, A and Pandit J.: Seasonal variation of spread-F occurrence probability at low
772 latitude and its relation with sunspot number. *International Journal of Electronics and*
773 *Communication technology* vol 5(2) pp. 40-43. 2014.

774 Bloomfield P.: Trends in global Temperature. *Climate Change*, 21:1-16,1992

775 Bloomfield P. and Nychka D.: Climate spectra and detecting climate change. *Climate Change*,
776 21:275-287,1992

777 Boon J., and C.Tsallis (Eds.): Nonextensive statistical mechanics: New trends, new
778 perspectives, *Europhys. News*, 36(6), 185 – 231. 2005

779 Burgula, L.F., A.F –Vixas, and C.Wang , Tsallis distribution of magnetic field strength variations
780 in the heliosphere: 5 to 90 AU, *J. Geophys. Res.*, 112, A07206, doi: 10.1029/2006
781 JA012213.2007

782 Chang, T., Low-Dimensional Behavior and Symmetry-Breaking of Stochastic-Systems Near
783 Criticality-Can These Effects Be Observed in Space and in the Laboratory, *IEEE Trans. On*
784 *Plasma Sci.*, 20(6), 691– 694, 1992.

785 Chang, T.: Sporadic localized reconnection and multiscale intermittent turbulence in the
786 magnetotail, *AGU Monograph No. 104, Geospace Mass and Energy Flow*, (Eds) Horwitz, J. L.,
787 Gallagher, D. L., and Peterson, W. K., p. 193, (American Geophysical Union, Washington, D.
788 C.), 1998

789 Chang, T., Self-organized criticality, multi-fractal spectra, sporadic localized reconnections and
790 intermittent turbulence in the magnetotail, *Phys. of Plasmas*, 6(11), 4137–4145, 1999.

791

792 Chapman, S. C., Watkins, N. W., Dendy, R. O., Helander, P., and Rowlands, G.: A simple
793 avalanche model as an analogue for magnetospheric activity, *Geophys. Res. Lett.*, 25, 2397–
794 2400, 1998.

795 Coco I., Consolini, G., Amata, E., Marcucci, M.F., Ambrosino.: Dynamical changes in polar cap
796 potential structure: an information theory approach. *Nonlinear processes in geophysics.*, 18, 697-
797 707, 2011.

798 Consolini, G., Marcucci, M. F., and Candidi, M.: Multifractal structure of auroral electrojet index
799 data, *Phys. Rev. Lett.*, 76 (21), 4082–4085, 1996.

800 Coraddu, M.; Lissia, M.; Tonelli, R. Statistical descriptions of nonlinear systems at the onset of
801 chaos arXiv:cond-mat/0511736v1 30 Nov 2005 2005

802 Cosolini, G., Chang, T.: Magnetic field topology and criticality in geotail dynamics relevance to
803 substorm phenomena. *Space Science Reviews* 95, 309-321, 2001.

804 DasGupta, A., Das, A.: Ionospheric total electron content (TEC) studies with GPS in the
805 equatorial region, *India journal of Radio and space Physics* 36,278-292.2007.

806 Fraser A.M. and Swinney H.L.: independent coordinates for storage attractors from mutual
807 information, *Phys.Rev,A*, 33, 1134 – 1141, 1986.

808 Freeman, M. P., and N. W. Watkins, The heavens in a pile of sand, *Science*, 298, 979– 980, (1
809 November), 2002.

810 Fuller- Rowell, T.J., Codrescu, M.V., Moffett, R.J. Quegan, S.: Response of the magnetosphere
811 and ionosphere to geomagnetic storms. *Journal of geophysical Research* 99, 3893-3914, 1994.

812 Hegger R., Kantz, H., Shreiber,T.: Practical implementation of nonlinear time series method. The
813 Tisean package, *Chaos*.9, 413 – 430. 1994

814 Kantz, H. and Shreiber, T.: *Nonlinear time series analysis*. Cambridge university press pp. 69-70,
815 2nd Ed. 2003.

816 Kazimirovsky, E.S. and Vergasova, G.V., *Mesospheric, Lower Thermospheric Dynamics and*
817 *External Forcing Effects: A Review*, *Indian J. Radio Space Phys.*, vol. 38, no. 1, pp. 7–36, 2009.

818 Kazimirovsky, E.S., Kokourov, V.D., and Vergasova, G.V., *Dynamical Climatology of the*
819 *Upper Mesosphere, Lower Thermosphere and Ionosphere*, *Surv. Geophys.*, vol. 27, pp. 211–255,
820 2006.

821 Kennel, M.B., Brown, R., and Abarbanel, H.D.I.: Determining minimum embedding dimension
822 using a geometrical construction, *Phys. Rev. A*, 45, 3403 – 3411, 1992.

823 Kim S, Koh, K., Boyd S., and Gorivesky D.: L_1 Trend filtering. *SIAM Review*, 51(2):339-360,
824 2009.

825 Klobuchar, J.: Design and characteristics of the GPS ionospheric time-delay algorithm for single
826 frequency users, in: Proceedings of PLANS'86 – Position Location and Navigation Symposium,
827 Las Vegas, Nevada, 280–286, 4–7 November 1986.

828 Kozelov, B. V. and Kozelova, T. V.: Sandpile model analogy of the magnetosphere-ionosphere
829 substorm activity, Proc. Interball Meeting, Warsaw, Poland, 2001.

830

831 Kumar, K.S., Kumar, C.V.A., George, B., Renuka, G., and Venugopal, C.: Analysis of the
832 fluctuations of the total electron content, measured at Goose Bay using tools of nonlinear
833 methods, *J. Geophys. Res.*, 10, A02308, doi: 10.1029/2002/A009768, 2004.

834 Lui, A.T.Y.: Evaluation on the analogy between the dynamic magnetosphere and a forced and/or
835 self-organised critical system. *Nonlin. Process in Geophys.* 9: 399-407, 2002.

836 Mukherjee, S., Shivalika, S., Purohit, P. K., and Gwal, A. K.: Study of GPS ionospheric
837 scintillations over equatorial anomaly station Bhopal. *International Journal of Advances in Earth*
838 *Science*. Vol 1 (2). Pp. 39-48, 2002.

839 Ogunsua B. O., Laoye J. A., Fuwape I. A., Rabiou A. B.: The comparative study of chaoticity and
840 dynamical complexity in the equatorial/ low latitude region of the ionosphere over Nigeria
841 during quiet and disturbed days. *Nonlin process in Geophys* vol. 21, 127-142, 2014.

842 Pavlos, G.P., Kyriakov, G.A., Rigas, A.G., Liatsis, P.I., Trochoulos, P.C., and Tsonis, A.A.:
843 Evidence for strange attractor structures in space plasma, *Ann. Geophys.*, 10, 309 – 315, 1992,
844 <http://www.ann-geophys.net/10/309/1992/>

845 Perreault, P. and Akasofu, S.-I.: A study of geomagnetic storms, *Geophys. J. R. Astron. Soc.*, 54,
846 547–573, 1978.

847 Rabiou, A. B., Mamukuyomi, A. I., Joshua, E. O.: Variability of equatorial ionosphere inferred
848 from geomagnetic field measurement, Bull. Astro Soc. India. 35, 607-615. India. 2007

849 Rama Rao, P.V.S., Gopi Krishna, S., Niranjana, K., and Prasad, D.S.V.V.D.: Temporal and
850 Spatial variations in TEC using simultaneous measurements from the India GPS network of
851 receivers during the low solar activity period of 2004/2005, Ann. Geophys., 24; 3279 – 3292,
852 doi: 10.5194/angeo-24-3279-2006, 2006.

853 Reddy D. S., Reddy N. G., Radhadevi P. V., Saibaba J., and Varadan G.: Peakwise smoothing of
854 data models using wavelets. *World Academy of Science, Engineering and Technology*, Vol:4
855 2010 03-24.

856 Remya, R., Unnikrishnan, K.: Chaotic Behaviour of interplanetary magnetic field under various
857 geomagnetic conditions. *Journal of atmospheric and solar terrestrial Physics*, 72, 662-675, 2010.

858 Rosenstein, M.T., Collins, J.J., DeLuca, C.J.: A practical method for calculation Largest
859 Lyapunov Exponents from small Data sets. *Physica D*. 65, 117, 1993.

860 Saito, A., Fukao, S., Mayazaki, S.: High resolution mapping of TEC perturbations with the GSI
861 GPS network over Japan. *Geophysical research letters*, 25, 3079-3082, 1998.

862 Savitzky A., Golay MJE, Smoothing and differentiation by simplified least square procedures.
863 *Analytical Chemistry* 1964, 36:1627-1639.

864 Shan, H., Hansen, P., Goertz, C. K., and Smith, K. A.: Chaotic appearance of the ae index, *J.*
865 *Geophys Res.*, 18(2), 147–150, 1991.

866

867 Sindelarova T., Buresova and D., Chum J.: Observations of acoustic-gravity waves in the
868 ionosphere generated by severe tropospheric weather. *Studia Geophysica et Geodaetica*, Volume
869 53, Issue 3, pp 403-418 2009. DOI:10.1007/s11200-009-0028-4

870

871 Tsallis, C: Possible generalization of Boltzmann-Gibbs statistics *J.Stat.phys.*, 52, 487-497. 1988

872 Tsallis,C: Generalised entropy-based criterion for consistent testing. Phys.Rev.E., 58, 1442 –
873 1445. 1998

874 Tsallis, C: Nonextensive statistics: theoretical, experimental and computational evidences and
875 connections. *Braz. J. Phys.* [online]. vol.29, n.1, pp. 1-35. ISSN 0103-9733 1999.

876 Unnikrishnan K.,Saito,A., and Fukao,S.: Differences in magnetic storm and quiet ionospheric
877 deterministic chaotic behavior. GPS TEC Analyses,J. Geophys Res,111, A06304, doi:
878 10.1029/2005 JA011311, 2006a

879 Unnikrishnan, K., Saito, A., and Fukao, S.: Differences in day and night time ionosphere
880 determine chaotic behavior : GPS TEC Analyses, J. Geophys. Res, 111, A07310, doi:
881 10.1029/2005 JA011313, 2006b.

882 Unnikrishnan, K.: comparison of chaotic aspects of magnetosphere under various physical
883 conditions using AE index time series *Ann. Geophysicae.*, 26, 941-953, 2008.

884 Unnikrishnan, K. Ravindran, S.: A study on chaotic behavior of equatorial/ low latitude
885 ionosphere over indian subcontinent, using Gps –TEC time series, *J. Atmo. Sol,-Ter. Phy.*, 72,
886 1080 – 1089, 2010.

887 Unnikrishnan, K.: Comparative study of chaoticity of Equatorial/low latitude ionosphere over
888 Indian subcontinent during geomagnetically quiet and disturbed periods. *Non Linear Processes in*
889 *Geophys*, 26, 941-953, 2010.

890

891 Uritsky, V. M., Klimas A. J., and Vassiliadis D.,: Evaluation of spreading critical exponents
892 from the spatiotemporal evolution of emission regions in the nighttime aurora, *Geophys. Res.*
893 *Lett.*, 30(15), 1813, doi:10.1029/2002GL016556, 2003.

894

895 Vassiliadis, D.V., Sharma, A.S, Eastman, T.E., and Papadopoulos,K.: Low –dimensionless chaos
896 in magnetospheric activity from AE time series, *Geophys, Res, let.*, 17, 1841 – 1844, 1990.

897 Vyas, R. M., and Dayanandan B.: Night time VHF ionospheric scintillation characteristics near
898 crest of Appleton anomaly stations, Udaipur ($26^{\circ}N$ $73^{\circ}E$). Indian Journal of Radio and Space
899 physics. Vol 40 (4) pp. 191-202, 2011.

900 Vyas, G. D., and Chandra, H.: VHF scintillations and spread-F in the anomaly crest region.
901 Indian Journal of Radio and Space physics. Vol 23 pp. 157-164, 1994.

902 Wernik, A.W. and Yeh,K.C: Chaotic behavior of ionospheric scintillation modelling and
903 observations, Radio Sci., 29, 135 – 139, 1994.

904 Wolf, A., Swift,J.B, Swinney, H.L, and Vastano,J.A. : Determining Lyapunov exponents from a
905 time series, Physica D, 16, 285 – 317, doi: 10.1016/0167 -2789 (85) – 90011-9, 1985.

906

907

908

909

910

911

912

913

914

915

916

917

918

919

920 Table 1: Coordinates of the GPS stations

Station Name	Geographic Coordinates		Dip latitude ($^{\circ}N$)
	Long ($^{\circ}E$)	Lat($^{\circ}N$)	
Birnin Kebbi	$4^{\circ} 12' E$	$12^{\circ} 32' N$	$0.62^{\circ} N$
Torro	$9^{\circ} 04' E$	$10^{\circ} 03' N$	$-0.82^{\circ} N$
Yola	$12^{\circ} 30' E$	$9^{\circ} 12' N$	$-1.39^{\circ} N$
Lagos	$3^{\circ} 23' E$	$6^{\circ} 27' N$	$-3.07^{\circ} N$
Enugu	$7^{\circ} 30' E$	$6^{\circ} 26' N$	$-3.21^{\circ} N$

928 Table 2a : Results of Surrogate data test for Lyapunov exponent for TEC data for the quietest
 929 days of October 2011 at Birnin Kebbi station.

Original Data	Surrogate data
0.1165	0.3921 ± 0.0420
0.0931	0.2029 ± 0.0756
0.1041	0.3860 ± 0.0741
0.0498	0.2891 ± 0.0598
0.1420.	0.3621 ± 0.0504

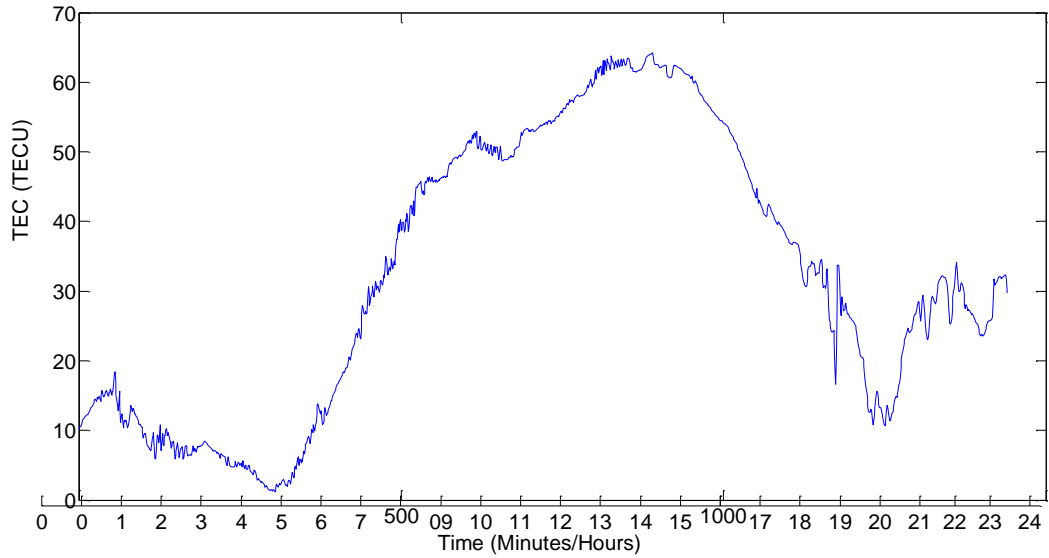
930

931 Table 2b: Results of Surrogate data test for Lyapunov exponent for TEC data for the most
 932 disturbed days of October 2011 at Birnin Kebbi station.

Original Data	Surrogate data
0.0579	0.3039 ± 0.0541
0.0502	0.3156 ± 0.0428
0.0786	0.2527 ± 0.0296
0.1795	0.3662 ± 0.0468
0.1038	0.3100 ± 0.0416

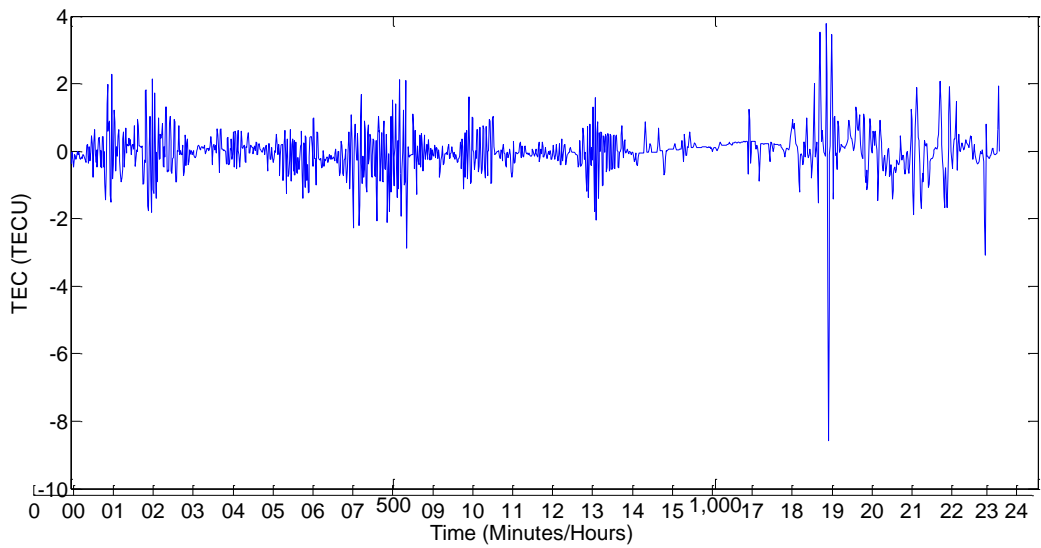
937

938



939

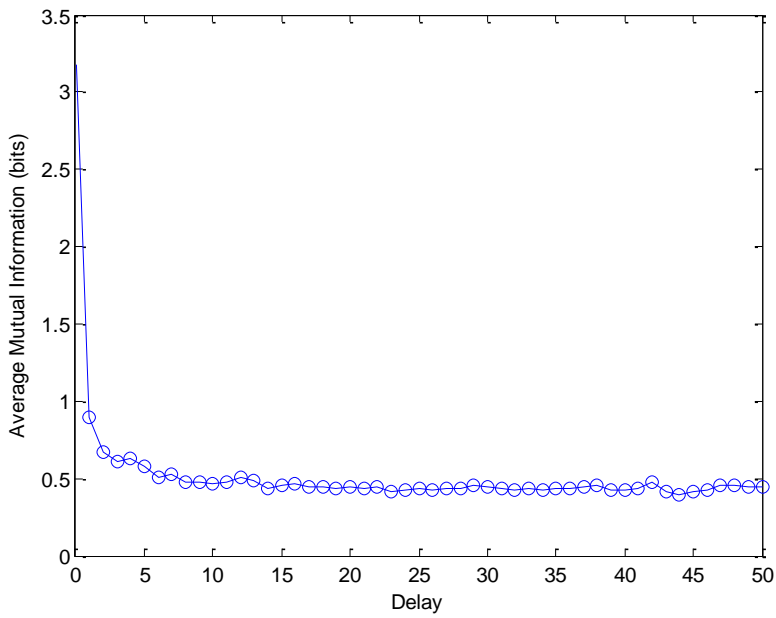
940 Fig 1. A typical time series plot for TEC measured at Lagos for 20 November 2011



941

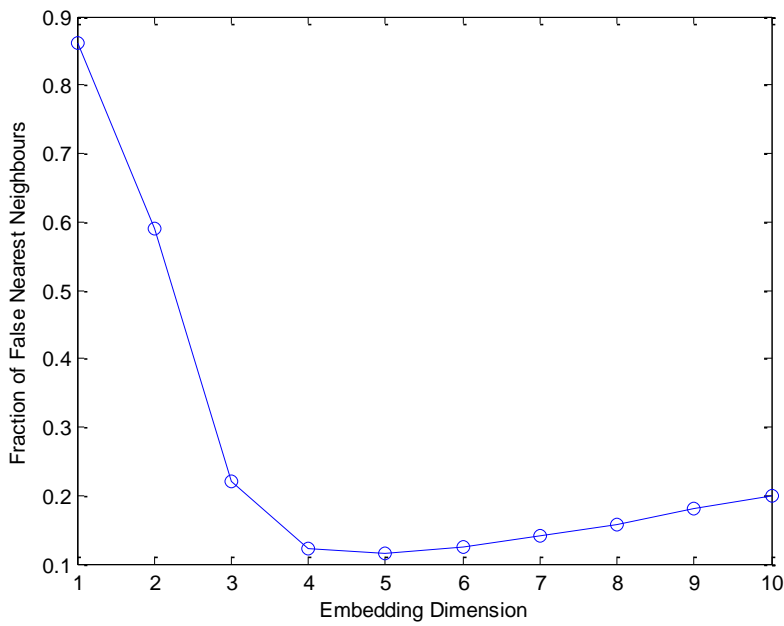
942 Fig 2. The detrended time series plot for TEC measured at Lagos

943



944

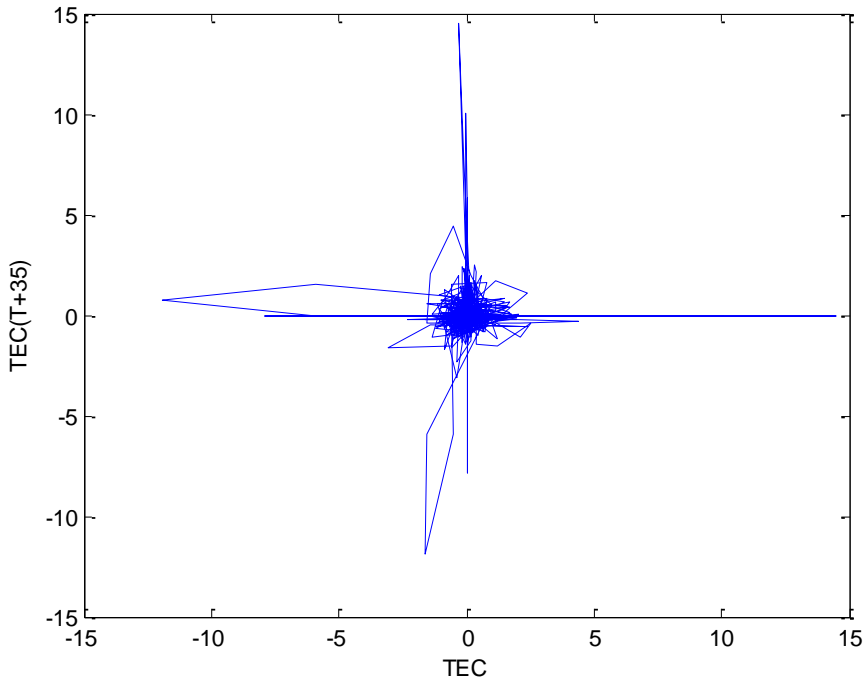
945 Fig. 3 Average mutual information against time Delay for TEC measured at Yola



946

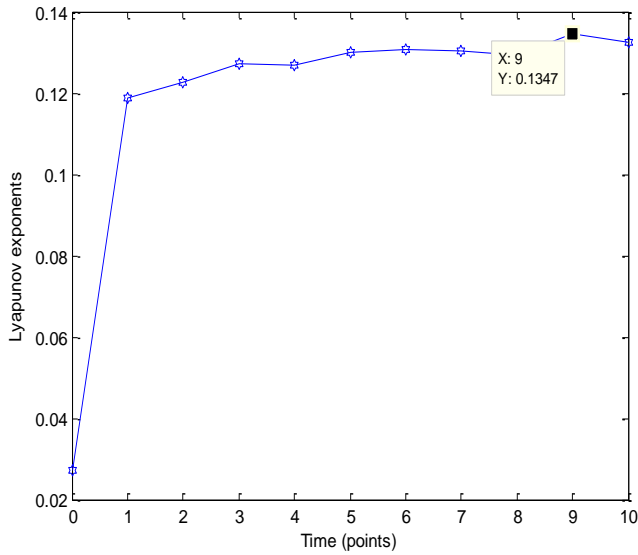
947 Fig. 4 Fraction of false nearest neighbours against embedding dimension for TEC measured at
 948 yola

949



950

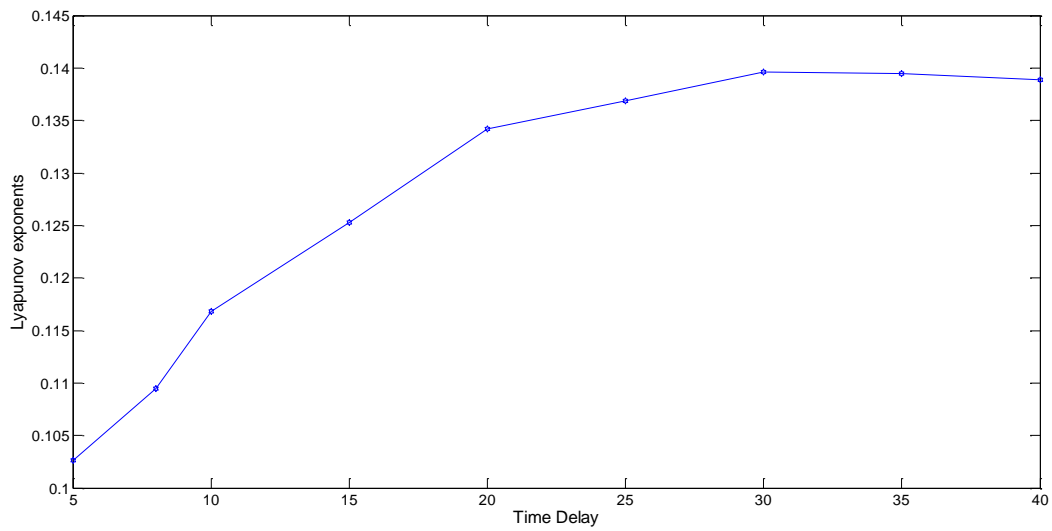
951 Fig.5 The Delay representation of the phase space reconstruction of the detrended TEC



952

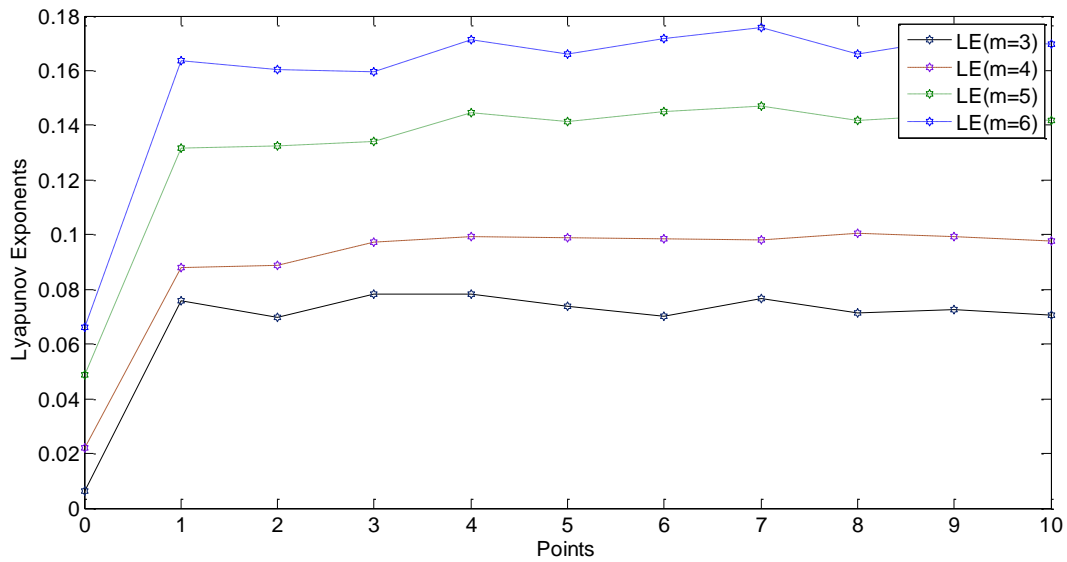
953 Fig. 6 Lyapunov Exponent computed and its evolution, computed as the state space trajectory
 954 scanned with $\tau=30$, $m=5$ for detrended time series measured at Yola with Largest Lyapunov
 955 Exponent equal to 0.1347.

956



957

958 Fig. 6b Lyapunov exponent computed for different time delay with a constant embedding
959 dimension.



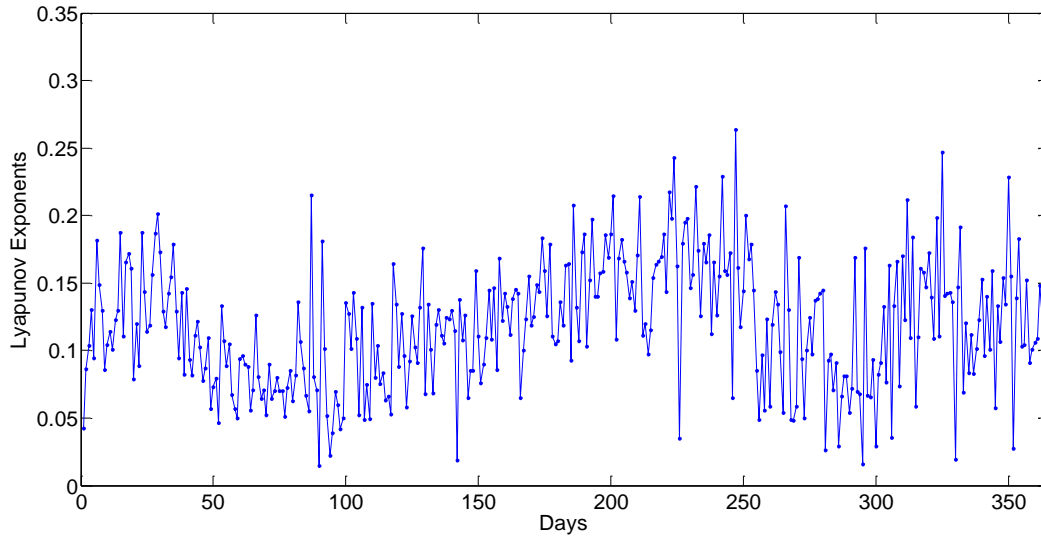
960

961 Fig. 6c Lyapunov exponents (LE) computed for different embedding dimension (m= 3,4,5 and 6)
962 at constant time delay

963

964

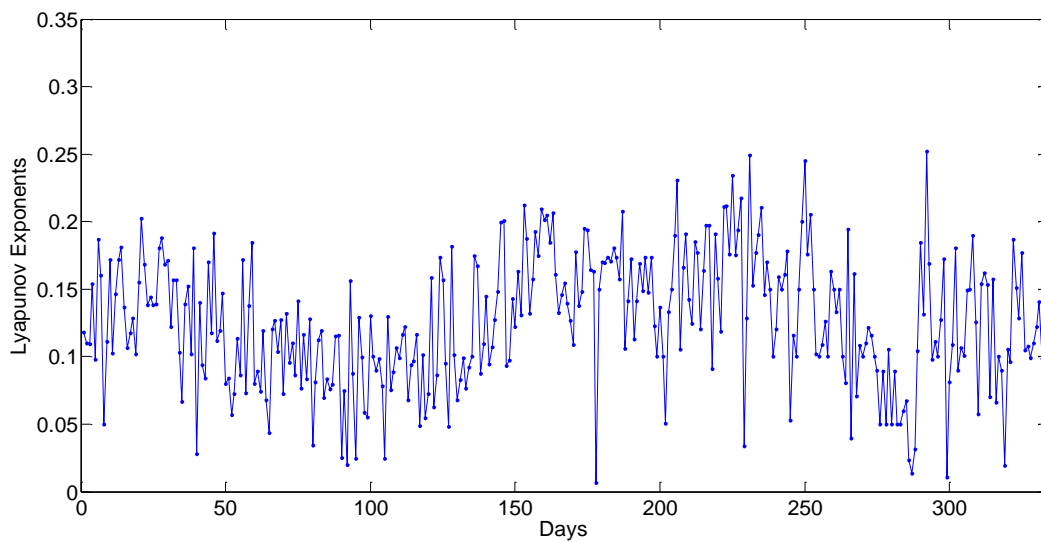
965



966

967 Fig. 7a The transient variations of Lyapunov exponents for 365 days of 2011 for detrended TEC
968 measured at Enugu

969

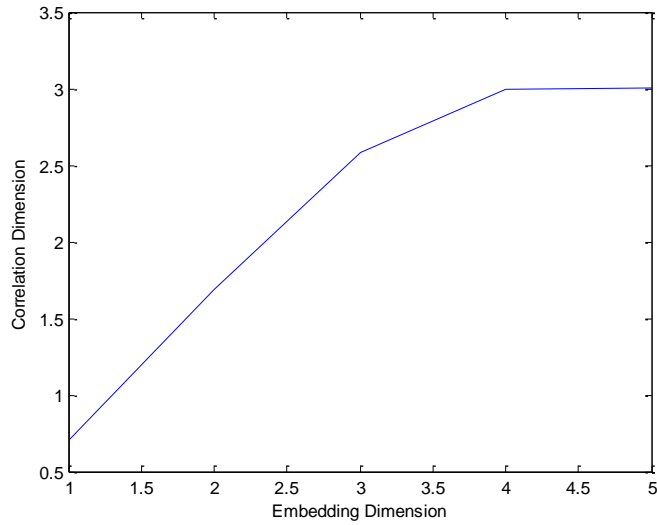


970

971 Fig. 7b The transient variations of Lyapunov exponents for 334 days (Jan 1 –Nov30) of 2011 for
972 detrended TEC measured at Toro

973

974

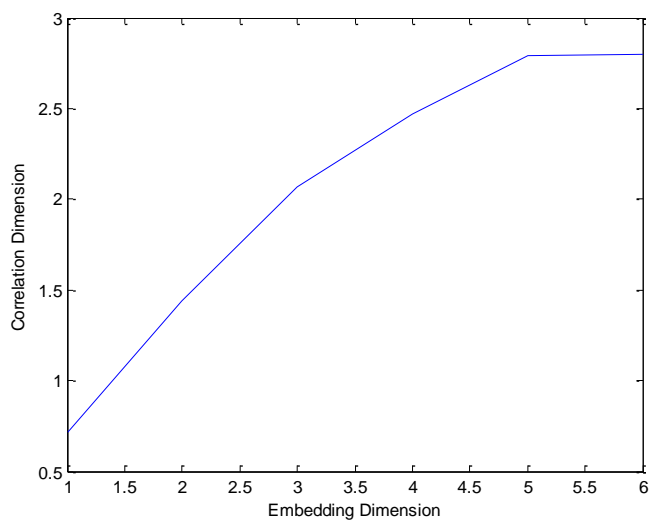


975

976 Fig. 8a The correlation dimension of the detrended TEC for the quietest day of October at Birnin

977 Kebbi which saturates at $m \geq 4$ and $\tau = 39$

978

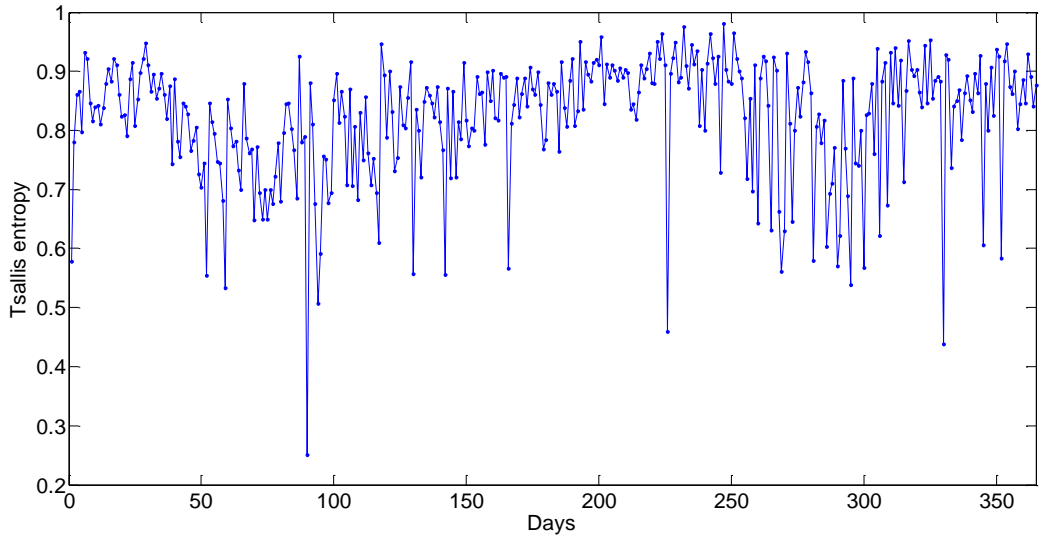


979

980

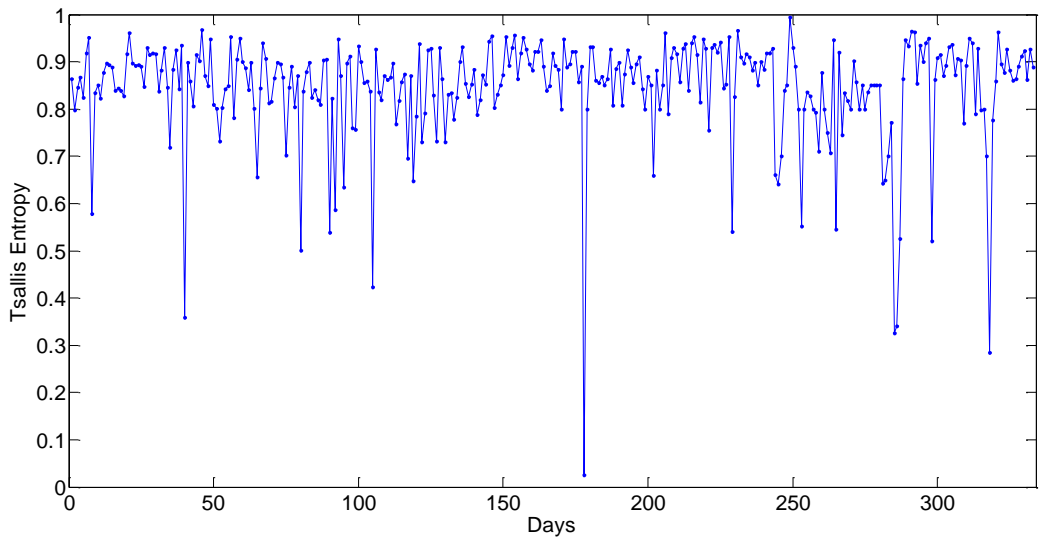
981 Fig. 8b The correlation dimension of the detrended for the most disturbed day of October at
982 Birnin Kebbi which saturates at $m \geq 5$ and $\tau = 34$

983



984

985 Fig. 9a The transient variations of Tsallis Entropy for 365 days (Jan1 –Nov30) of 2011 for
986 detrended TEC measured at Enugu

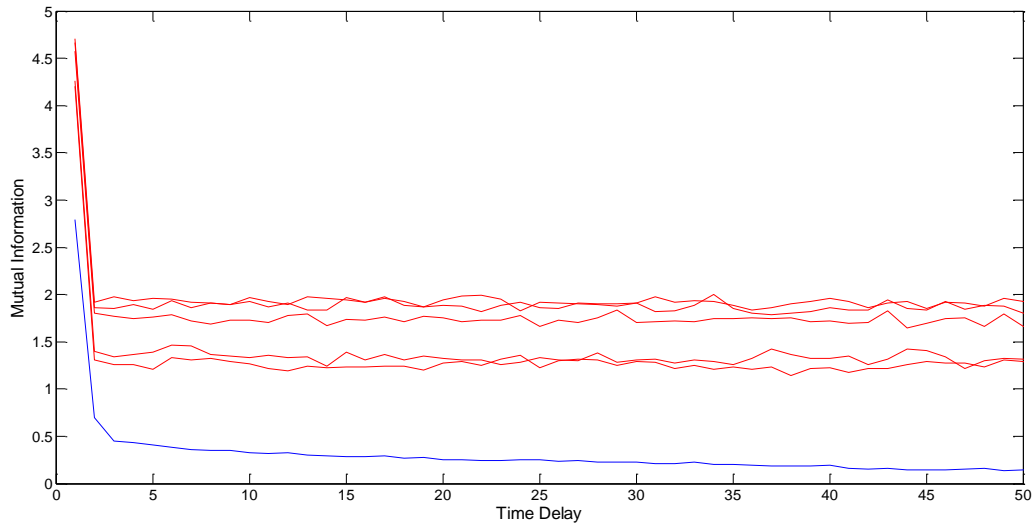


987

988 Fig. 9b The transient variations of Tsallis Entropy for 334 days (Jan1 –Nov30) of 2011 for
989 detrended TEC measured at Toro

990

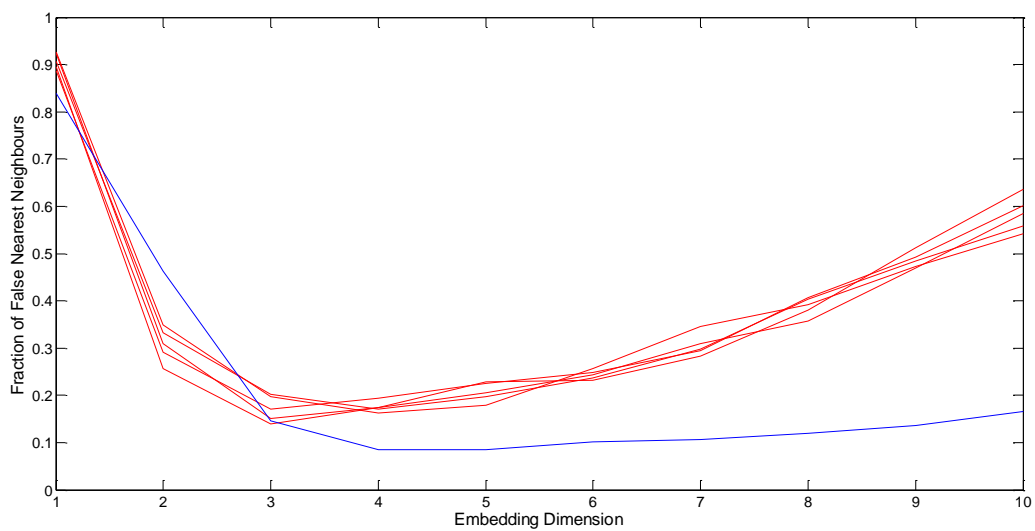
991



992

993 Fig 10 Mutual information plotted against time delay for the original detrended data in (blue
994 curve) with the mutual information for the surrogate data (red curve) for TEC data measured at
995 Lagos for the quietest day of march 2011

996

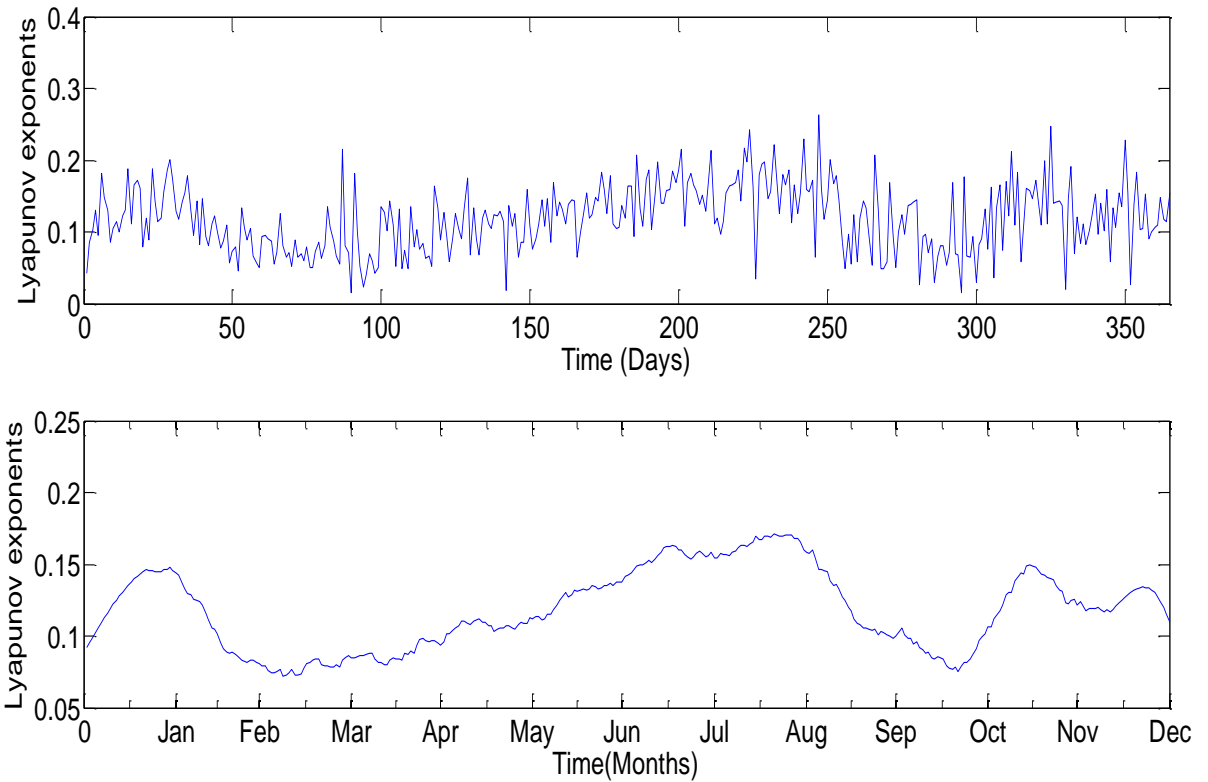


997

998 Fig 11 Fraction of false nearest neighbours plotted against time embedding dimension for the
999 original detrended data in (blue curve) with the mutual information for the surrogate data (red
1000 curve) for TEC data measured at Lagos for the quietest day of march 20

1001

1002



1003

1004 Fig. 12a Daily variation of Lyapunov exponents for TEC measured at the Enugu station for the
1005 year 2011 showing the Original data (Upper Panel) and the smoothed Plot of daily variation of
1006 Lyapunov exponents for TEC measured at the Enugu station for the year 2011 (Lower panel)

1007

1008

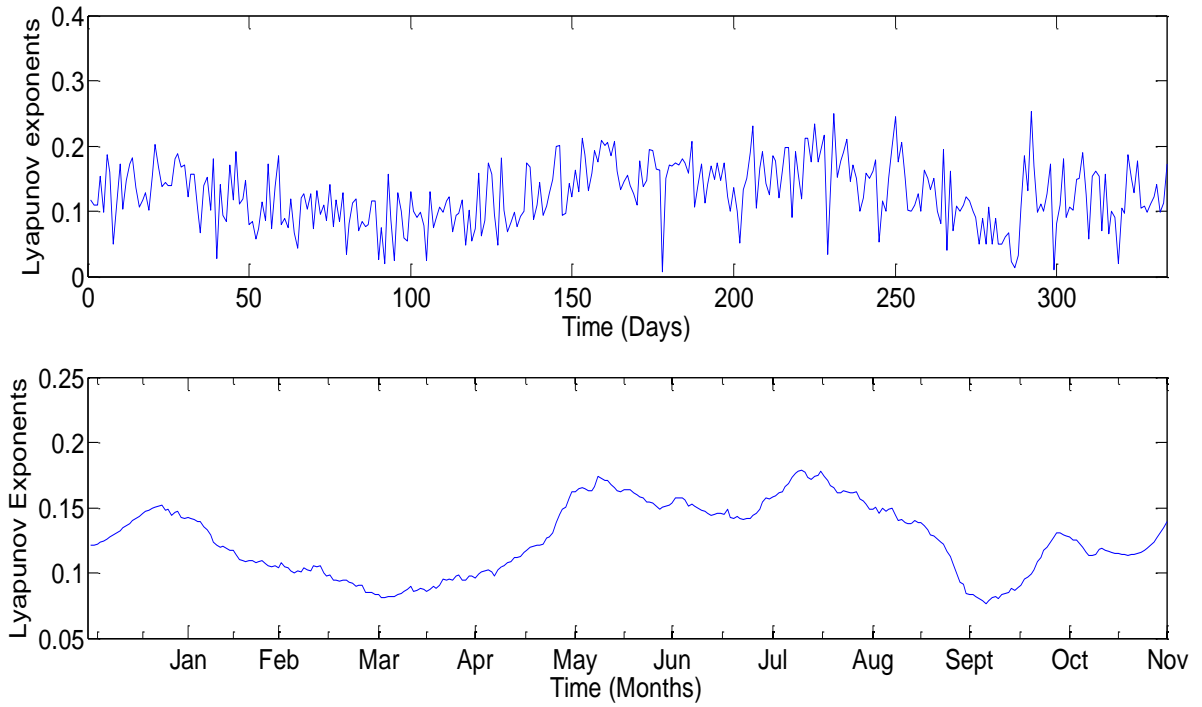
1009

1010

1011

1012

1013



1014

1015

1016 Fig 12b Daily variation of Lyapunov exponents for TEC measured at the Toro station for the
1017 year 2011 showing the Original data (Upper Panel) and the smoothed Plot of daily variation of
1018 Lyapunov exponents for TEC measured at the Toro station for the year 2011 (Lower panel)

1019

1020

1021

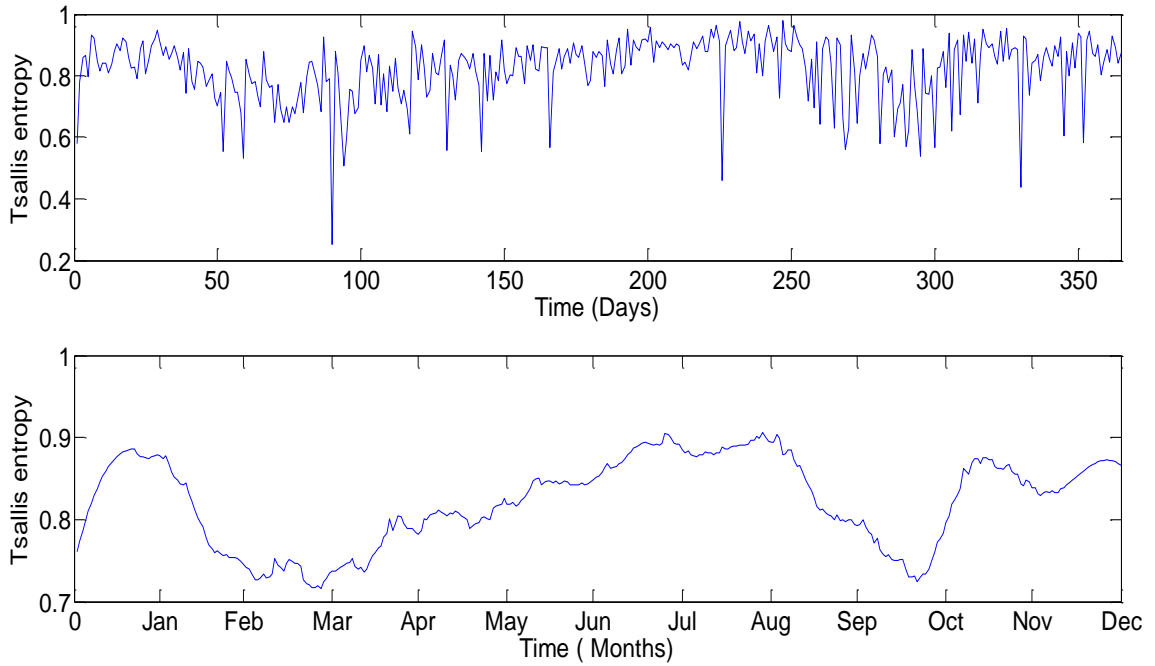
1022

1023

1024

1025

1026



1027

1028 Fig. 13a Daily variation of Tsallis entropy for TEC measured at the Enugu station for the year
1029 2011 showing the Original data (Upper Panel) and the smoothed Plot of daily variation of
1030 Lyapunov exponents for TEC measured at the Enugu station for the year 2011 (Lower panel)

1031

1032

1033

1034

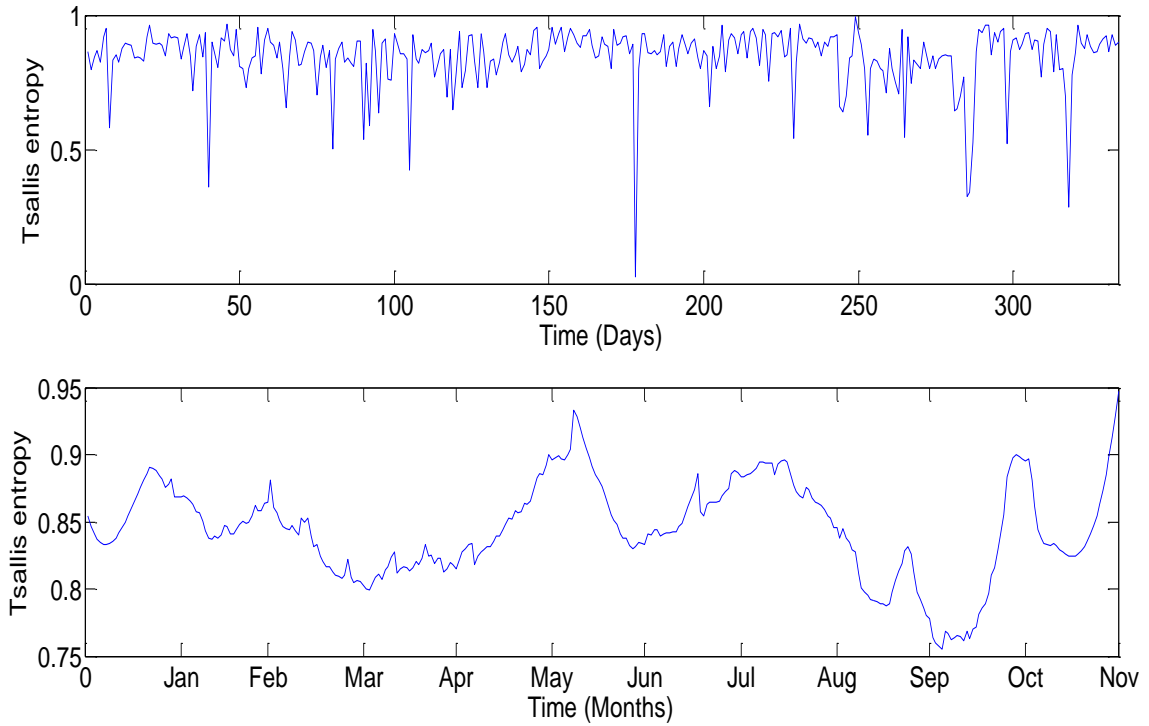
1035

1036

1037

1038

1039



1040

1041

1042 Fig. 13b Daily variation of Tsallis entropy for TEC measured at the Toro station for the year
1043 2011 showing the Original data (Upper Panel) and the smoothed Plot of daily variation of
1044 Lyapunov exponents for TEC measured at the Enugu station for the year 2011 (Lower panel)

1045

1046

1047

1048

1049

1050

1051

1052